Science Advances
AAAS

advances.sciencemag.org/cgi/content/full/6/2/eaax4001/DC1

Supplementary Materials for

Widespread activation of developmental gene expression characterized by PRC1-dependent chromatin looping

V. Loubiere, G. L. Papadopoulos, Q. Szabo, A-M. Martinez*, G. Cavalli*

*Corresponding author. Email: anne-marie.martinez@igh.cnrs.fr (A-M.M.); giacomo.cavalli@igh.cnrs.fr (G.C.)

Published 10 January 2020, *Sci. Adv.* **6**, eaax4001 (2020)
DOI: 10.1126/sciadv.aax4001

The PDF file includes:

Other Supplementary Material for this manuscript includes the following:

(available at advances.sciencemag.org/cgi/content/full/6/2/eaax4001/DC1)

Table S1 (Microsoft Excel format). Chromatin types from *Drosophila* ED.
Table S2 (Microsoft Excel format). Gene ontologies of the top interacting aTSS bins identified on the basis of PH ChIP-seq enrichment.
Table S3 (Microsoft Excel format). Stringent set of PRC1 peak summits used for the clustering in ED.
Table S4 (Microsoft Excel format). List of the genes assigned to each cluster of PRC1 peaks in ED.
Table S5 (Microsoft Excel format). FPKM of *Drosophila* genes for the different conditions used in this study.
Table S6 (Microsoft Excel format). Comparative Gene Ontology analysis of the genes assigned to each cluster of PRC1 peaks in ED.
Table S7 (Microsoft Excel format). Differential gene expression analyses during development and in polycomb mutant Eds.
Table S8 (Microsoft Excel format). List of the antibodies used in the study.
Table S9 (Microsoft Excel format). PCR primers used in the study.
Table S10 (Microsoft Excel format). NGS datasets used in the study.

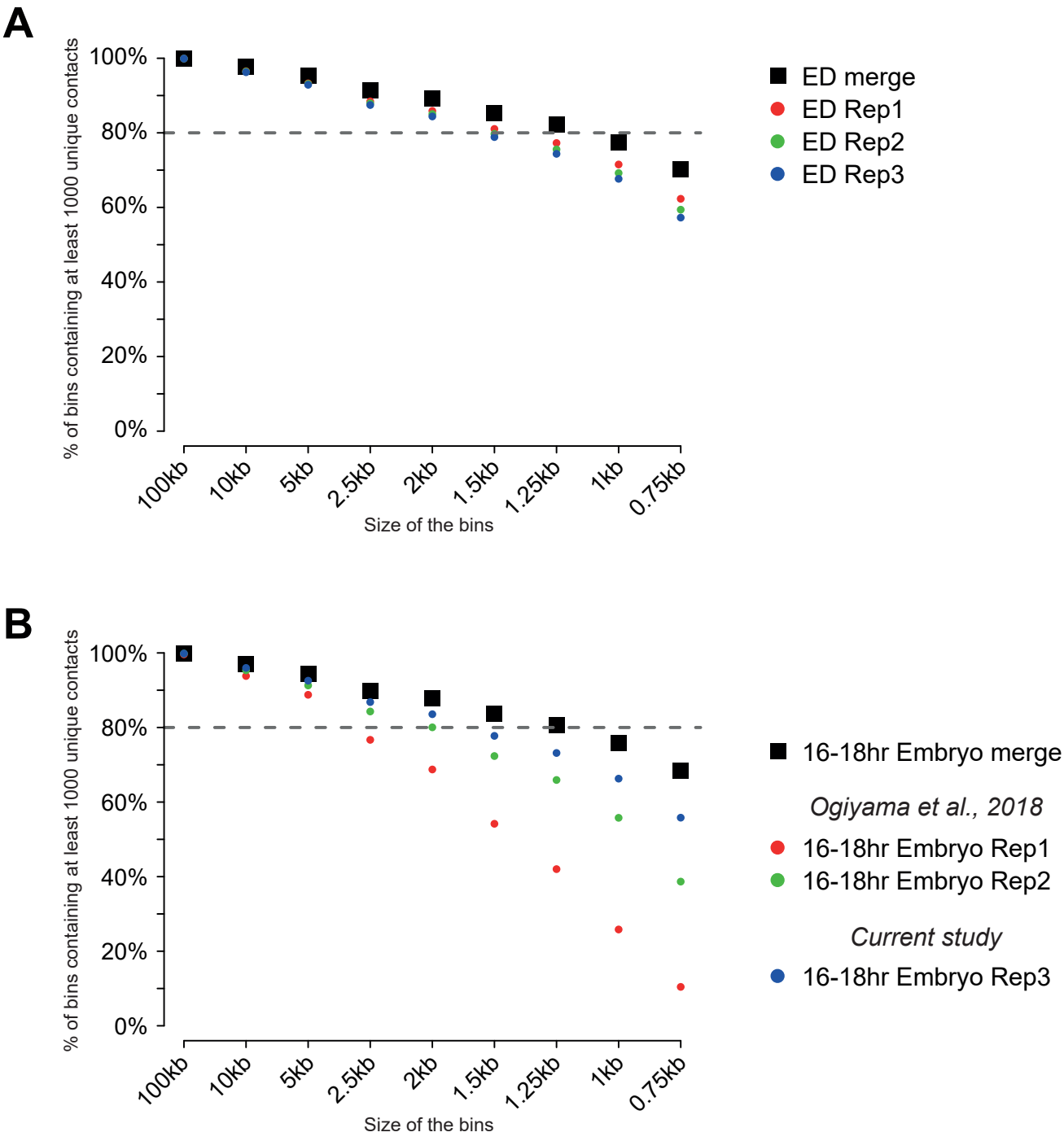
A
100%
80%
60%
40%
20%
0%
% of bins containing at least 1000 unique contacts
100kb
10kb
5kb
2.5kb
2kb
1.5kb
1.25kb
1kb
0.75kb
Size of the bins
ED merge
ED Rep1
ED Rep2
ED Rep3
B
100%
80%
60%
40%
20%
0%
% of bins containing at least 1000 unique contacts
100kb
10kb
5kb
2.5kb
2kb
1.5kb
1.25kb
1kb
0.75kb
Size of the bins
16-18hr Embryo merge
Ogiyama et al., 2018
16-18hr Embryo Rep1
16-18hr Embryo Rep2
Current study
16-18hr Embryo Rep3

Figure S1

Fig. S1. Resolution of Hi-C maps. The resolution of Hi-C maps is defined as the minimum bin size such that 80% of the bins contain at least 1,000 unique contacts. **A-** The merged map from ED reaches a ~1.25kb resolution. **B-** We supplemented (blue dot) pre-existing Hi-C data (Ogiyama et al., 2018; red and green dots) generated with the same protocol from late 16-18h embryo to achieve a comparable resolution of ~1.25kb after merging the replicates.

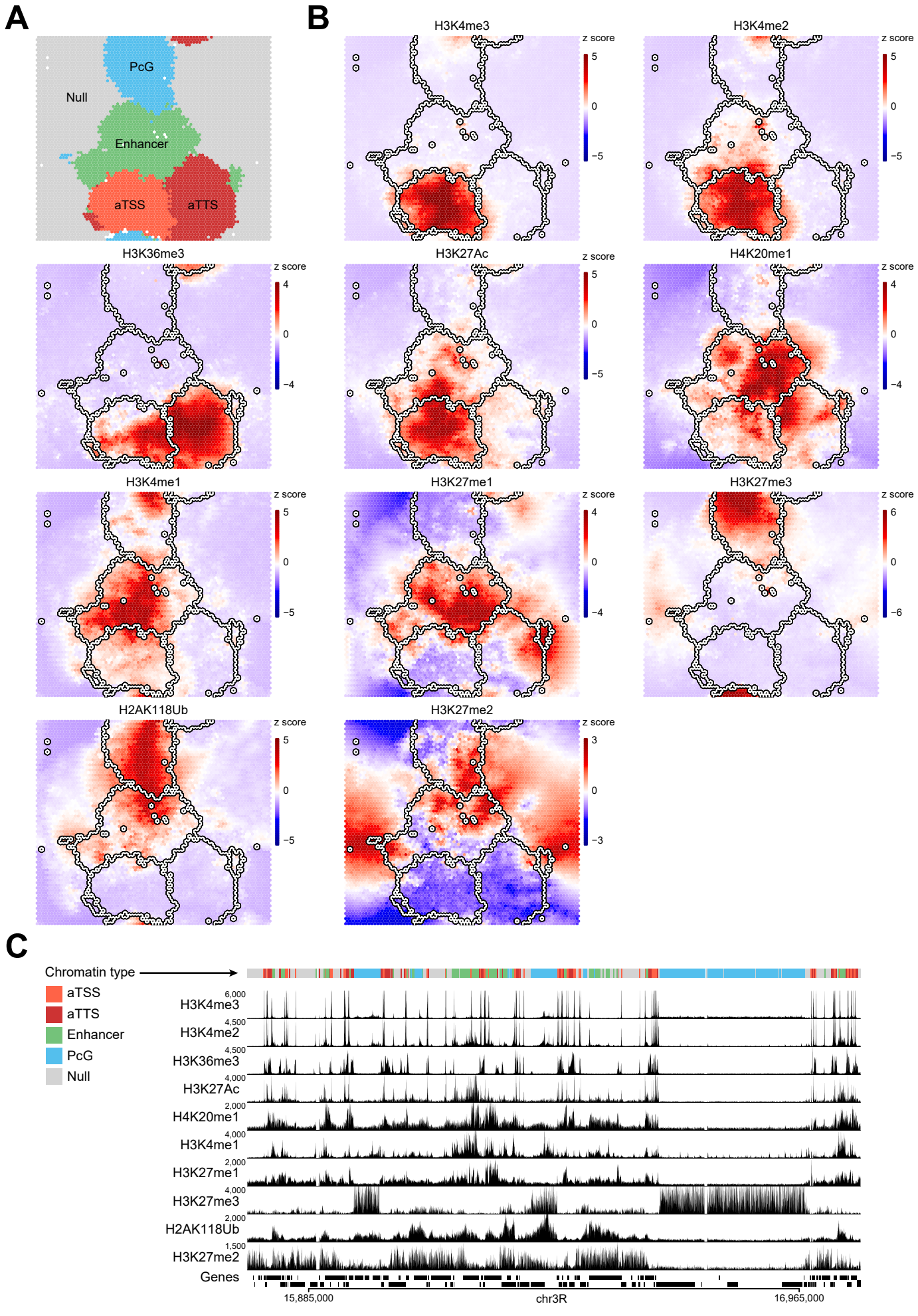
A
PcG
Null
Enhancer
aTSS
aTTS
B
H3K4me3
H3K4me2
H3K36me3
H3K27Ac
H4K20me1
H3K4me1
H3K27me1
H3K27me3
H2AK118Ub
H3K27me2
z score
C
Chromatin type
aTSS
aTTS
Enhancer
PcG
Null
H3K4me3
H3K4me2
H3K36me3
H3K27Ac
H4K20me1
H3K4me1
H3K27me1
H3K27me3
H2AK118Ub
H3K27me2
Genes
15,885,000
chr3R
16,965,000

Figure S2

Fig. S2. SOMs of 10 PTM ChIP-seq from ED. To stratify the ED epigenome genome-wide irrespectively of PcG binding, we used unsupervised clustering using Self-Organizing Maps (SOMs), which is a powerful method to identify complex relationships between genomic data (Mortazavi et al., 2013, see Material and Methods). **A-** To facilitate the visualization and the quantification of the maps, we over-imposed a k-mean clustering on the map nodes (k=5). The resulting clusters exhibit the hallmarks of active Transcription Start Sites (aTSS, in red) and Transcription Termination Sites (aTTS, in dark red), Enhancers (in green), PcG-repressed (in blue) and Null chromatin (in grey). **B-** For each PTM used for the training (see the title of each map), the resulting map is shown. In such maps, a given genomic bin always ends up in the same node, and the color of the node indicates the mean z-score of all the bins assigned to it (color scales are shown on the right). Hence, these maps can be compared side by side to identify broad, but also more subtle relationships between PTMs at a genome-wide level. Interestingly, although the H3K27me3 mark is restricted to the PcG cluster (top center of the map), the PRC1-mediated H2AK118Ub mark shows a different pattern and leaks into the Enhancer cluster (center of the map). Conversely, the H3K4me1 enhancer mark is also enriched at a subset of PcG bins. **C-** Screenshot of the ChIP-Seq tracks used for the clustering (~1.4Mb region on the chromosome 3R). Corresponding stratification into 5 chromatin types is shown on the top part (see legend on the left).

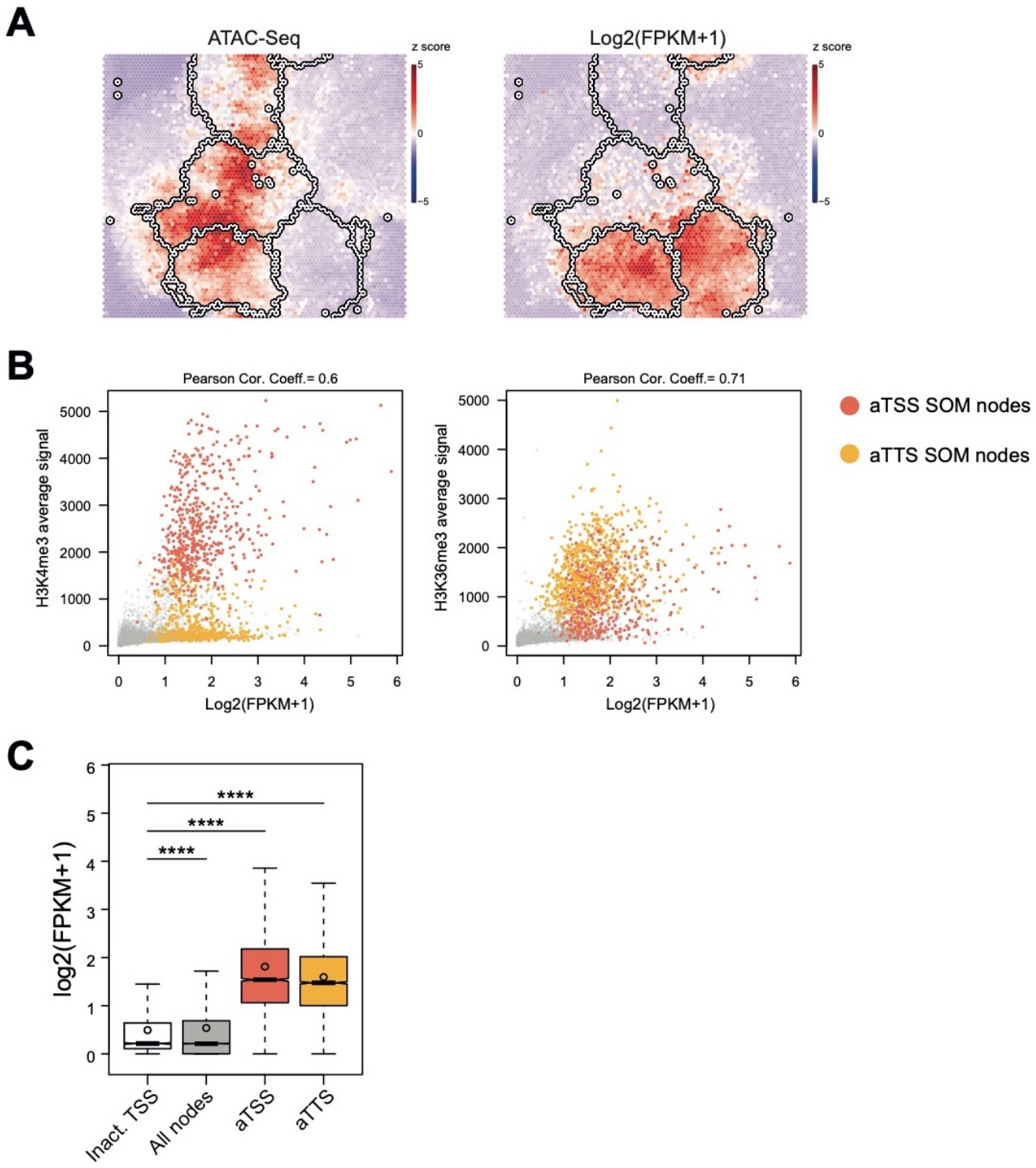
A
ATAC-Seq
z score
5
0
−5
Log2(FPKM+1)
z score
5
0
−5
B
Pearson Cor. Coeff.= 0.6
H3K4me3 average signal
5000
4000
3000
2000
1000
0
0
1
2
3
4
5
6
Log2(FPKM+1)
Pearson Cor. Coeff.= 0.71
H3K36me3 average signal
5000
4000
3000
2000
1000
0
0
1
2
3
4
5
6
Log2(FPKM+1)
aTSS SOM nodes
aTTS SOM nodes
C
log2(FPKM+1)
6
5
4
3
2
1
0
****
****
****
Inact. TSS
All nodes
aTSS
aTTS

Fig. S3. aTSS and aTSS SOM clusters are transcriptionally active. A- SOM maps showing the repartition of ATAC-Seq (on the left) and RNA-Seq (on the right) signals (see fig. S2A). High levels of ATAC-Seq are found at aTSS and Enhancer bins, as expected. In addition, a subset of PcG nodes also show consistent ATAC-Seq enrichment. Finally, the majority of highly transcribed nodes correspond to aTSS and aTTS clusters, as expected, while PcG nodes are transcriptionally silent. **B-** Scatterplots showing the correlation between the mean RNA-Seq (Log2(FPKM+1)) and H3K4me3 (on the left) or H3K36me3 (on the right) levels in the ED. **C-** Boxplot of the RNA-Seq levels (Log2(FPKM+1)) within all SOM nodes (grey), aTSS bins (orange) and aTTS bins (yellow). As a control, the RNA-Seq levels at annotated TSSs that do not overlap with aTSS bins are shown in white (Inact. TSS). Wilcoxon p.val: **** < 1E-05.

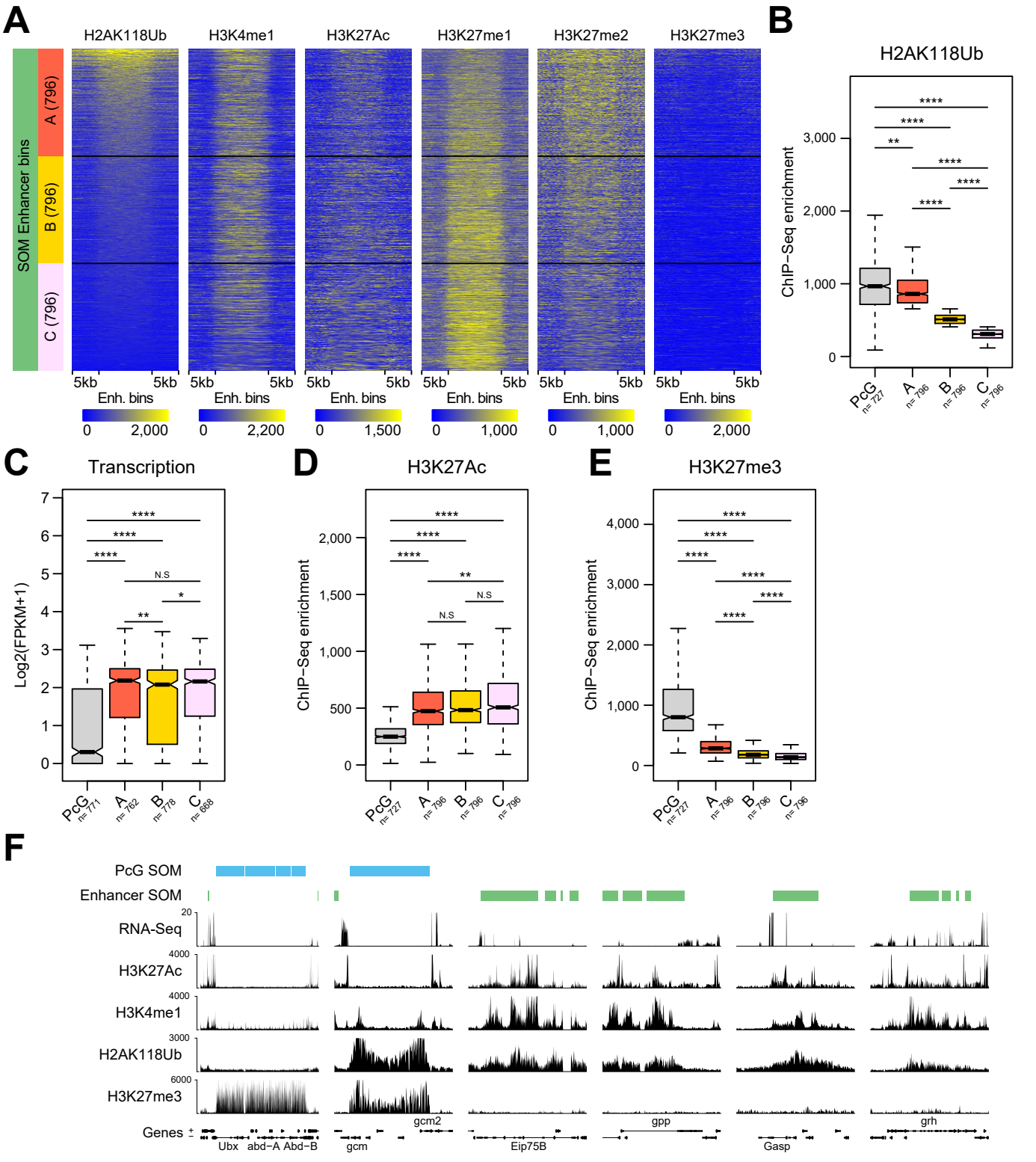
A
H2AK118Ub
H3K4me1
H3K27Ac
H3K27me1
H3K27me2
H3K27me3
SOM Enhancer bins
A (796)
B (796)
C (796)
5kb
Enh. bins
0
2,000
2,200
1,500
1,000
B
H2AK118Ub
ChIP−Seq enrichment
PcG n= 727
A n= 796
B n= 796
C n= 796
C
Transcription
Log2(FPKM+1)
PcG n= 771
A n= 762
B n= 778
C n= 668
D
H3K27Ac
E
H3K27me3
N.S
F
PcG SOM
Enhancer SOM
RNA-Seq
H3K27Ac
H3K4me1
H2AK118Ub
H3K27me3
Genes
Ubx
abd−A
Abd−B
gcm
gcm2
Eip75B
gpp
Gasp
grh

Figure S4

Fig. S4. A subset of active enhancers shows substantial H2AK118Ub enrichment in the ED. A- Anchored heatmaps showing the enrichment for the H2AK118Ub PRC1 mark, H3K4me1, H3K27Ac, H3K27me1, H3K27me2 and the H3K27me3 PRC2 mark within merged enhancer bins (+/- 5kb). Merged enhancer bins were segmented into 3 quantiles named A (H2AK118Ub++, in orange), B (H2AK118Ub+, in yellow) and C (H2AK118Ub-, in pink). The clusters and corresponding numbers are depicted on the left. **B-E-** Quantification of H2AK11Ub (B), RNA-Seq (Log2(FPKM+1) (C), H3K27Ac (D) and H3K27me3 (E) levels at PcG bins and the 3 (A, B and C) enhancer clusters. While the A cluster contains high levels of H2AK118Ub, overlapping genes show comparable transcriptional and H3K27Ac levels compared to the clusters B (H2AK118Ub+) and C (H2AK118Ub-). Moreover, H3K27me3 levels at cluster A enhancers remain significantly lower compared to PcG bins. Wilcoxon p.val: **** < 1E-05; *** < 1E-03; ** < 1E-02; * < 5E-02; N.S: Not Significant. **F-** Screenshots of RNA-Seq, H3K27Ac, H3K4me1, H2AK118Ub and H3K27me3 genomic tracks at selected regions. While the PcG-repressed bithorax complex is transcriptionally silent and shows high H3K27me3 levels without any H2AK118Ub enrichment, the *gcm*/*gcm2* locus shows high H2AK118Ub levels together with sharp H3K4me1 peaks. Finally, the *Eip75B*, *Gasp* and *grh* locus are devoid of H3K27me3 and transcriptionally active, while also exhibiting substantial H2AK118Ub enrichment.

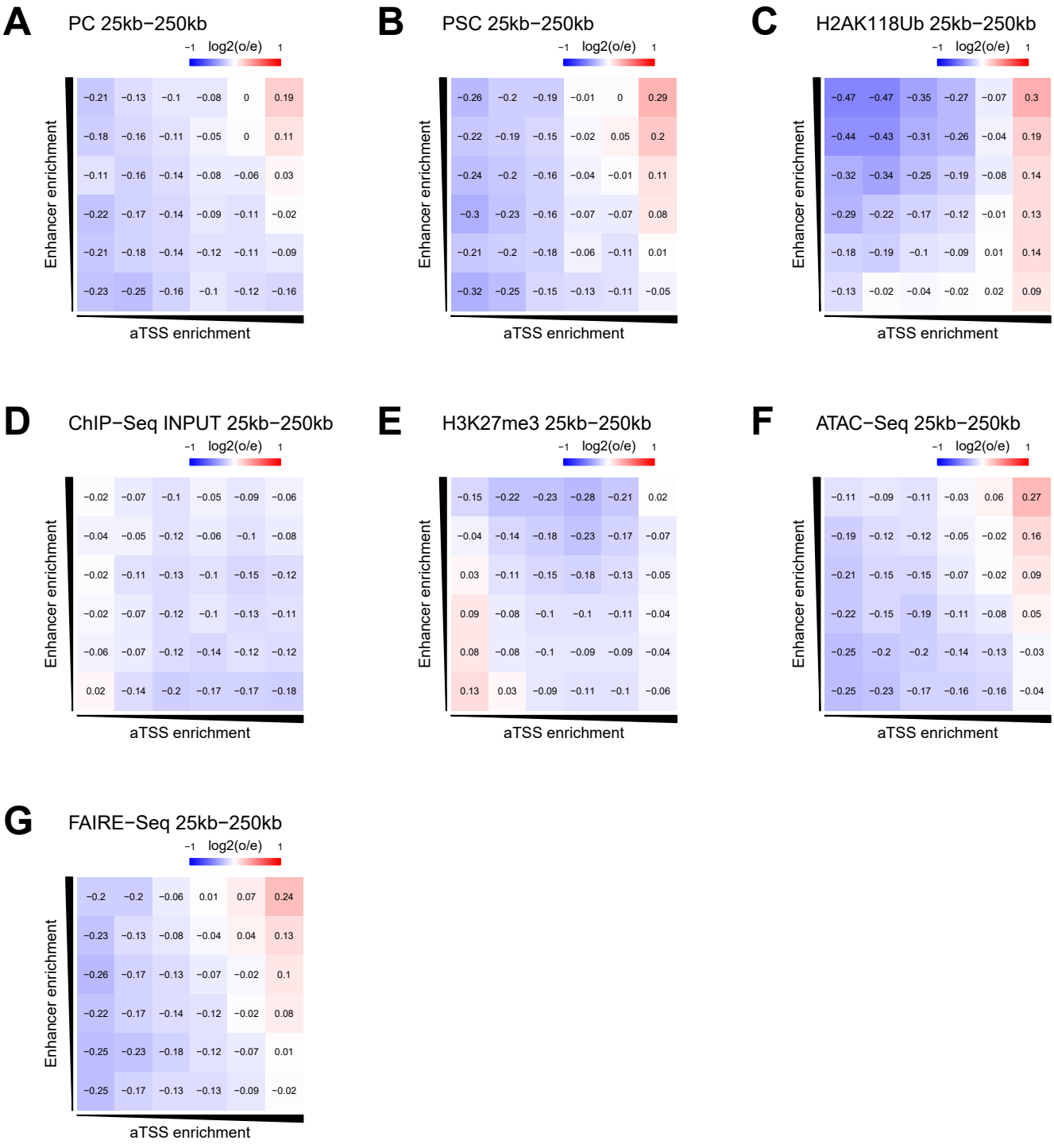
A
PC 25kb−250kb
−1 log2(o/e) 1
−0.21 −0.13 −0.1 −0.08 0 0.19
−0.18 −0.16 −0.11 −0.05 0 0.11
−0.11 −0.16 −0.14 −0.08 −0.06 0.03
−0.22 −0.17 −0.14 −0.09 −0.11 −0.02
−0.21 −0.18 −0.14 −0.12 −0.11 −0.09
−0.23 −0.25 −0.16 −0.1 −0.12 −0.16
Enhancer enrichment
aTSS enrichment
B
PSC 25kb−250kb
−1 log2(o/e) 1
−0.26 −0.2 −0.19 −0.01 0 0.29
−0.22 −0.19 −0.15 −0.02 0.05 0.2
−0.24 −0.2 −0.16 −0.04 −0.01 0.11
−0.3 −0.23 −0.16 −0.07 −0.07 0.08
−0.21 −0.2 −0.18 −0.06 −0.11 0.01
−0.32 −0.25 −0.15 −0.13 −0.11 −0.05
Enhancer enrichment
aTSS enrichment
C
H2AK118Ub 25kb−250kb
−1 log2(o/e) 1
−0.47 −0.47 −0.35 −0.27 −0.07 0.3
−0.44 −0.43 −0.31 −0.26 −0.04 0.19
−0.32 −0.34 −0.25 −0.19 −0.08 0.14
−0.29 −0.22 −0.17 −0.12 −0.01 0.13
−0.18 −0.19 −0.1 −0.09 0.01 0.14
−0.13 −0.02 −0.04 −0.02 0.02 0.09
Enhancer enrichment
aTSS enrichment
D
ChIP−Seq INPUT 25kb−250kb
−1 log2(o/e) 1
−0.02 −0.07 −0.1 −0.05 −0.09 −0.06
−0.04 −0.05 −0.12 −0.06 −0.1 −0.08
−0.02 −0.11 −0.13 −0.1 −0.15 −0.12
−0.02 −0.07 −0.12 −0.1 −0.13 −0.11
−0.06 −0.07 −0.12 −0.14 −0.12 −0.12
0.02 −0.14 −0.2 −0.17 −0.17 −0.18
Enhancer enrichment
aTSS enrichment
E
H3K27me3 25kb−250kb
−1 log2(o/e) 1
−0.15 −0.22 −0.23 −0.28 −0.21 0.02
−0.04 −0.14 −0.18 −0.23 −0.17 −0.07
0.03 −0.11 −0.15 −0.18 −0.13 −0.05
0.09 −0.08 −0.1 −0.1 −0.11 −0.04
0.08 −0.08 −0.1 −0.09 −0.09 −0.04
0.13 0.03 −0.09 −0.11 −0.1 −0.06
Enhancer enrichment
aTSS enrichment
F
ATAC−Seq 25kb−250kb
−1 log2(o/e) 1
−0.11 −0.09 −0.11 −0.03 0.06 0.27
−0.19 −0.12 −0.12 −0.05 −0.02 0.16
−0.21 −0.15 −0.15 −0.07 −0.02 0.09
−0.22 −0.15 −0.19 −0.11 −0.08 0.05
−0.25 −0.2 −0.2 −0.14 −0.13 −0.03
−0.25 −0.23 −0.17 −0.16 −0.16 −0.04
Enhancer enrichment
aTSS enrichment
G
FAIRE−Seq 25kb−250kb
−1 log2(o/e) 1
−0.2 −0.2 −0.06 0.01 0.07 0.24
−0.23 −0.13 −0.08 −0.04 0.04 0.13
−0.26 −0.17 −0.13 −0.07 −0.02 0.1
−0.22 −0.17 −0.14 −0.12 −0.02 0.08
−0.25 −0.23 −0.18 −0.12 −0.07 0.01
−0.25 −0.17 −0.13 −0.13 −0.09 −0.02
Enhancer enrichment
aTSS enrichment

Figure S5

Fig. S5. High levels of PRC1 and H2AK118Ub are associated with increased enhancer-promoter interaction frequencies at short-range distances (25 to 250 kb). Log2(observed/expected) average interaction frequencies between “aTSS” and “Enhancer” bins ranked by the strength of selected ChIP-Seq enrichments. **A-C-** Higher levels of the PRC1 proteins PC and PSC or the PRC1-mediated H2AK118Ub mark are associated with stronger enhancer-promoter contact frequencies at short-range distances (25kb-250kb). **D-E-** As a control, higher levels of ChIP-Seq INPUT or H3K27me3 are not associated with higher enhancer-promoter contact frequencies. Therefore, these contacts do not stem from canonical PRC1 binding sites enriched for H3K27me3. **F-G-** Higher chromatin openness, as measured by ATAC-Seq (Davie et al., 2015) or FAIRE-Seq (McKay et al., 2013), is also associated with higher contact frequencies between promoter and enhancer bins at short-range distances.

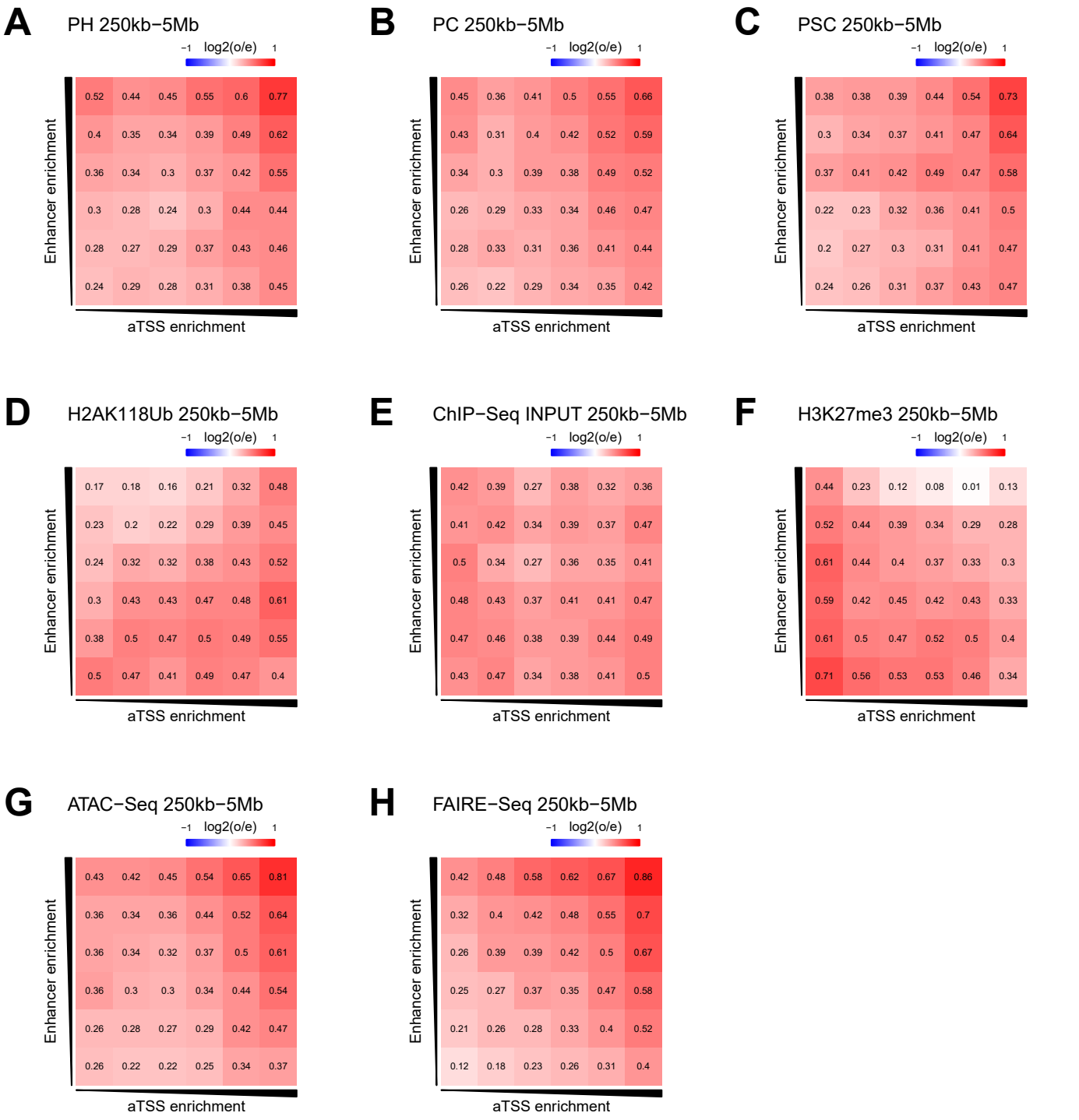
A
PH 250kb−5Mb
B
PC 250kb−5Mb
C
PSC 250kb−5Mb
D
H2AK118Ub 250kb−5Mb
E
ChIP−Seq INPUT 250kb−5Mb
F
H3K27me3 250kb−5Mb
G
ATAC−Seq 250kb−5Mb
H
FAIRE−Seq 250kb−5Mb
−1 log2(o/e) 1
Enhancer enrichment
aTSS enrichment

Figure S6

Fig. S6. High levels of PRC1 are associated with increased enhancer-promoter interaction frequencies at long-range distances (250 kb to 5 Mb). Log2(observed/expected) average interaction frequencies between "aTSS" and "Enhancer" bins ranked by the strength of selected ChIP-Seq enrichments. **A-C-** Higher levels of the PRC1 proteins PH, PC and PSC are associated with stronger enhancer-promoter contact frequencies at long-range distances (250kb-5Mb). **D-** In contrast with shorter range (fig. S5), the H2AK118Ub mark loses its predictive power for increased enhancer-promoter contact frequencies at long-range distances (250kb-5Mb). **E-F-** As a control, higher levels of ChIP-Seq INPUT or H3K27me3 are not associated with increased enhancer-promoter contact frequencies. **G-H-** Higher chromatin openness, as measured by ATAC-Seq (Davie et al., 2015) or FAIRE-Seq (McKay et al., 2013), is also associated with higher contact frequencies between promoter and enhancer bins at long-range distances.

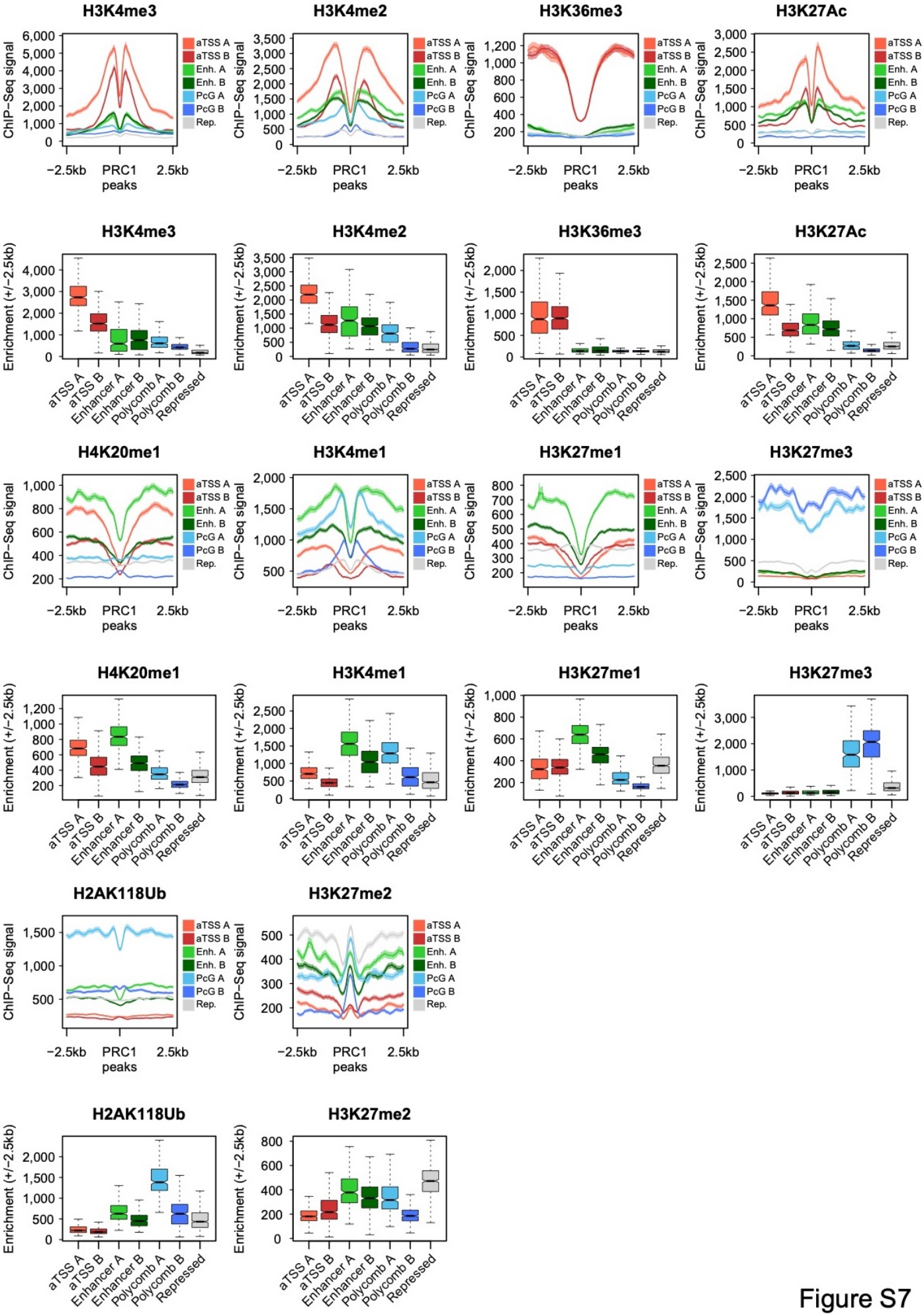
H3K4me3
H3K4me2
H3K36me3
H3K27Ac
ChIP−Seq signal
−2.5kb
PRC1 peaks
2.5kb
aTSS A
aTSS B
Enh. A
Enh. B
PcG A
PcG B
Rep.
Enrichment (+/−2.5kb)
aTSS A
aTSS B
Enhancer A
Enhancer B
Polycomb A
Polycomb B
Repressed
H4K20me1
H3K4me1
H3K27me1
H3K27me3
H2AK118Ub
H3K27me2

Figure S7

Fig. S7. Quantification of PTM ChIP-seq signal for each cluster of PRC1 peaks. Average PTM ChIP-Seq tracks (see the title of each chart) centered on the PRC1 peak summits of each cluster in ED (+/- 2.5kb, the legend is shown on the right). Below each average track, corresponding quantifications are shown.

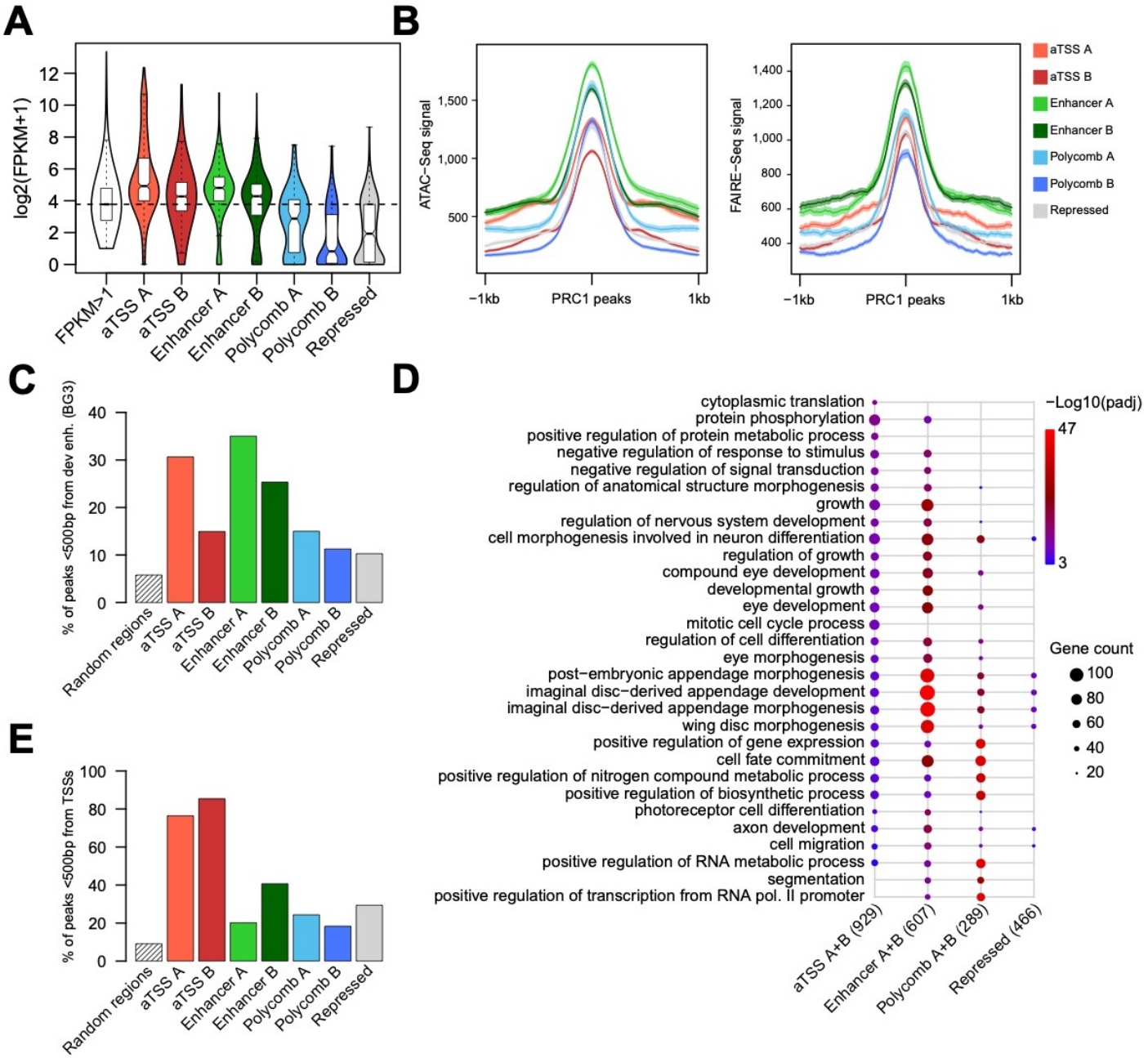
A
log2(FPKM+1)
FPKM>1
aTSS A
aTSS B
Enhancer A
Enhancer B
Polycomb A
Polycomb B
Repressed
B
ATAC−Seq signal
FAIRE−Seq signal
−1kb
PRC1 peaks
1kb
aTSS A
aTSS B
Enhancer A
Enhancer B
Polycomb A
Polycomb B
Repressed
C
% of peaks <500bp from dev enh. (BG3)
Random regions
D
cytoplasmic translation
protein phosphorylation
positive regulation of protein metabolic process
negative regulation of response to stimulus
negative regulation of signal transduction
regulation of anatomical structure morphogenesis
growth
regulation of nervous system development
cell morphogenesis involved in neuron differentiation
regulation of growth
compound eye development
developmental growth
eye development
mitotic cell cycle process
regulation of cell differentiation
eye morphogenesis
post−embryonic appendage morphogenesis
imaginal disc−derived appendage development
imaginal disc−derived appendage morphogenesis
wing disc morphogenesis
positive regulation of gene expression
cell fate commitment
positive regulation of nitrogen compound metabolic process
positive regulation of biosynthetic process
photoreceptor cell differentiation
axon development
cell migration
positive regulation of RNA metabolic process
segmentation
positive regulation of transcription from RNA pol. II promoter
aTSS A+B (929)
Enhancer A+B (607)
Polycomb A+B (289)
Repressed (466)
−Log10(padj)
Gene count
E
% of peaks <500bp from TSSs
Random regions

Figure S8

Fig. S8. PRC1 clusters have distinct genomic features. A- Violin plot of the log2(FPKM+1) of the genes assigned to each cluster in ED defined in Fig. 1H. **B-** Aggregate plots of ATAC-Seq (left) and FAIRE-Seq (right) signals centered on PRC1 peaks (+/- 1kb). The legend is shown on the right. **C-** Percentage of PRC1 peaks overlapping (<500bp) STARR-Seq developmental enhancers (dev enh., BG3 cells). **D**- Comparative Gene Ontology (GO) analysis of the genes assigned to each PRC1 cluster. **E-** Percentage of PRC1 peaks overlapping (<500bp) annotated Transcription Start Sites (TSSs).

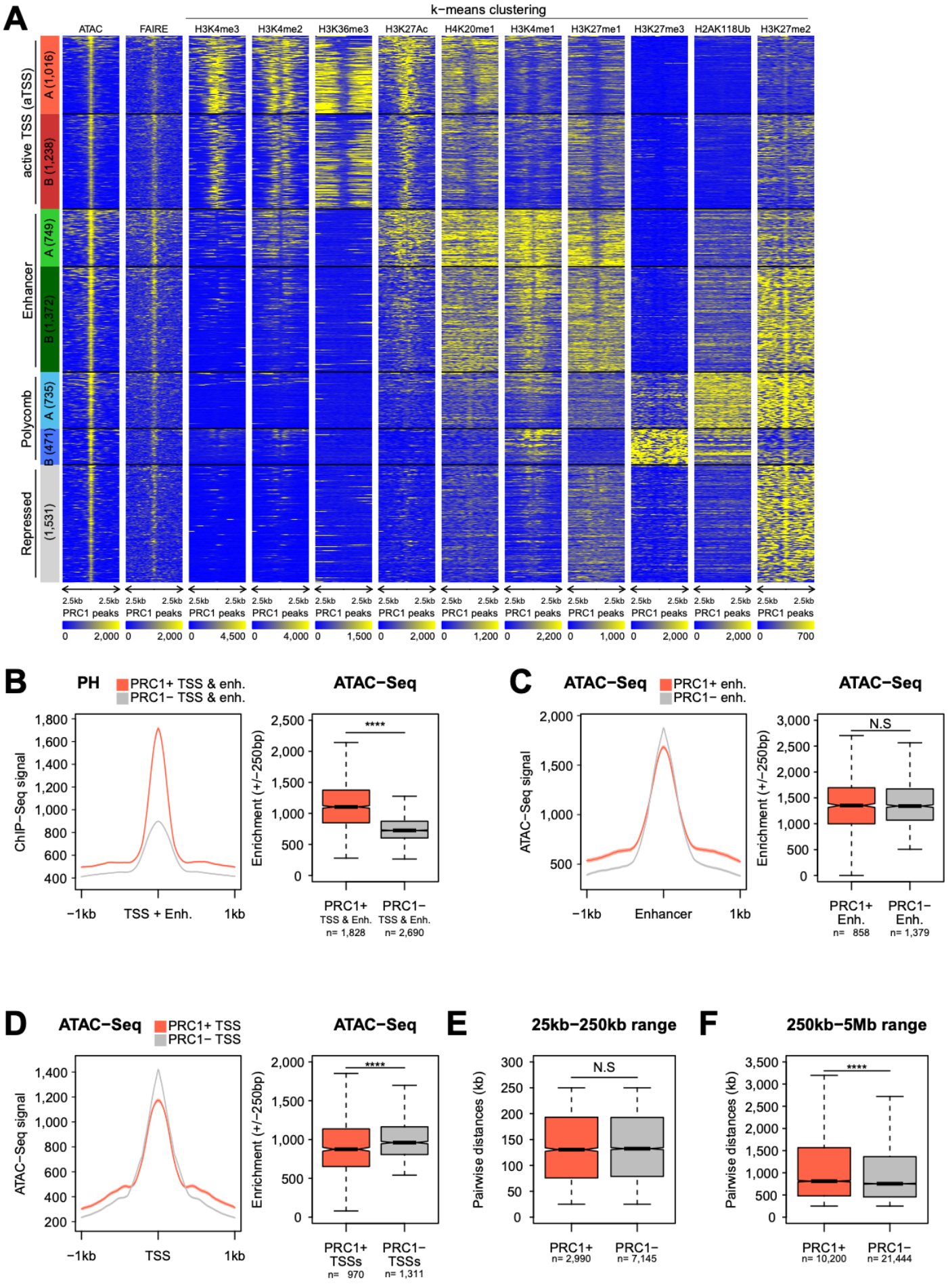
A
k−means clustering
ATAC
FAIRE
H3K4me3
H3K4me2
H3K36me3
H3K27Ac
H4K20me1
H3K4me1
H3K27me1
H3K27me3
H2AK118Ub
H3K27me2
active TSS (aTSS)
A (1,016)
B (1,238)
Enhancer
A (749)
B (1,372)
Polycomb
A (735)
B (471)
Repressed
(1,531)
2.5kb 2.5kb
PRC1 peaks
0 2,000
0 2,000
0 4,500
0 4,000
0 1,500
0 2,000
0 1,200
0 2,200
0 1,000
0 2,000
0 2,000
0 700
B
PH
PRC1+ TSS & enh.
PRC1− TSS & enh.
ChIP−Seq signal
1,800
1,600
1,400
1,200
1,000
800
600
400
−1kb
TSS + Enh.
1kb
ATAC−Seq
Enrichment (+/−250bp)
2,500
2,000
1,500
1,000
500
0
****
PRC1+
TSS & Enh.
n= 1,828
PRC1−
TSS & Enh.
n= 2,690
C
ATAC−Seq
PRC1+ enh.
PRC1− enh.
ATAC−Seq signal
2,000
1,500
1,000
500
−1kb
Enhancer
1kb
ATAC−Seq
Enrichment (+/−250bp)
3,000
2,500
2,000
1,500
1,000
500
0
N.S
PRC1+
Enh.
n= 858
PRC1−
Enh.
n= 1,379
D
ATAC−Seq
PRC1+ TSS
PRC1− TSS
ATAC−Seq signal
1,400
1,200
1,000
800
600
400
200
−1kb
TSS
1kb
ATAC−Seq
Enrichment (+/−250bp)
2,000
1,500
1,000
500
0
****
PRC1+
TSSs
n= 970
PRC1−
TSSs
n= 1,311
E
25kb−250kb range
Pairwise distances (kb)
300
250
200
150
100
50
0
N.S
PRC1+
n= 2,990
PRC1−
n= 7,145
F
250kb−5Mb range
Pairwise distances (kb)
3,500
3,000
2,500
2,000
1,500
1,000
500
0
****
PRC1+
n= 10,200
PRC1−
n= 21,444

Figure S9

Fig. S9. *k*-Means clustering of ED ATAC-seq peaks provides control sets of aTSSs and enhancers. Both promoters and enhancers are known to exhibit a nucleosome free region when active. Therefore, we used ATAC-Seq peaks from ED to identify control sets of active promoters and enhancers that are not bound by PRC1. **A-** Heatmap resulting from the k-means clustering of PTM ChIP-Seq around a stringent set of ATAC-Seq peaks from ED (+/- 2.5kb). This approach identifies sets of peaks with PTM signatures similar to PRC1-bound aTSSs (in orange and red) and enhancers (in lemon green and dark green). Finally, the ATAC-Seq aTSS and enhancer peak summits that do not overlap with highly confident PRC1 peak summits in ED (+/- 2.5kb) were used as control sets of PRC1-depleted (PRC1-) peaks. **B-** PH average ChIP-Seq tracks centered on PRC1-depleted (PRC1-, in grey) and PRC1-bound (PRC1+, in orange) TSS and enhancer sites (+/- 1kb). Correponsing quantifications of PH ChIP-Seq enrichment (+/- 250bp) are shown on the right panel. Wilcoxon p.val: **** < 1E-05. **C-D-** PRC1-depleted (PRC1-, in grey) enhancers (C) and TSSs (D) have comparable or slightly higher ATAC-Seq levels compared to PRC1-enriched enhancers and TSSs (PRC1+, in orange). **E-F-** Moreover, PRC1-depleted (PRC1-, in grey) and PRC1-bound (PRC1+, in orange) enhancer-promoter pairs show comparable pairwise short-range distances (E), while PRC1- pairs are closer at long-range distance (F). Therefore, PRC1-depleted aTSS and enhancer ATAC-Seq peaks are appropriate controls for addressing the impact of PRC1 binding on enhancer-promoter contact frequencies in Hi-C, since they will not be skewed neither by weaker chromatin openness nor by longer genomic distances. Wilcoxon p.val: **** < 1E-05; N.S: Not Significant.

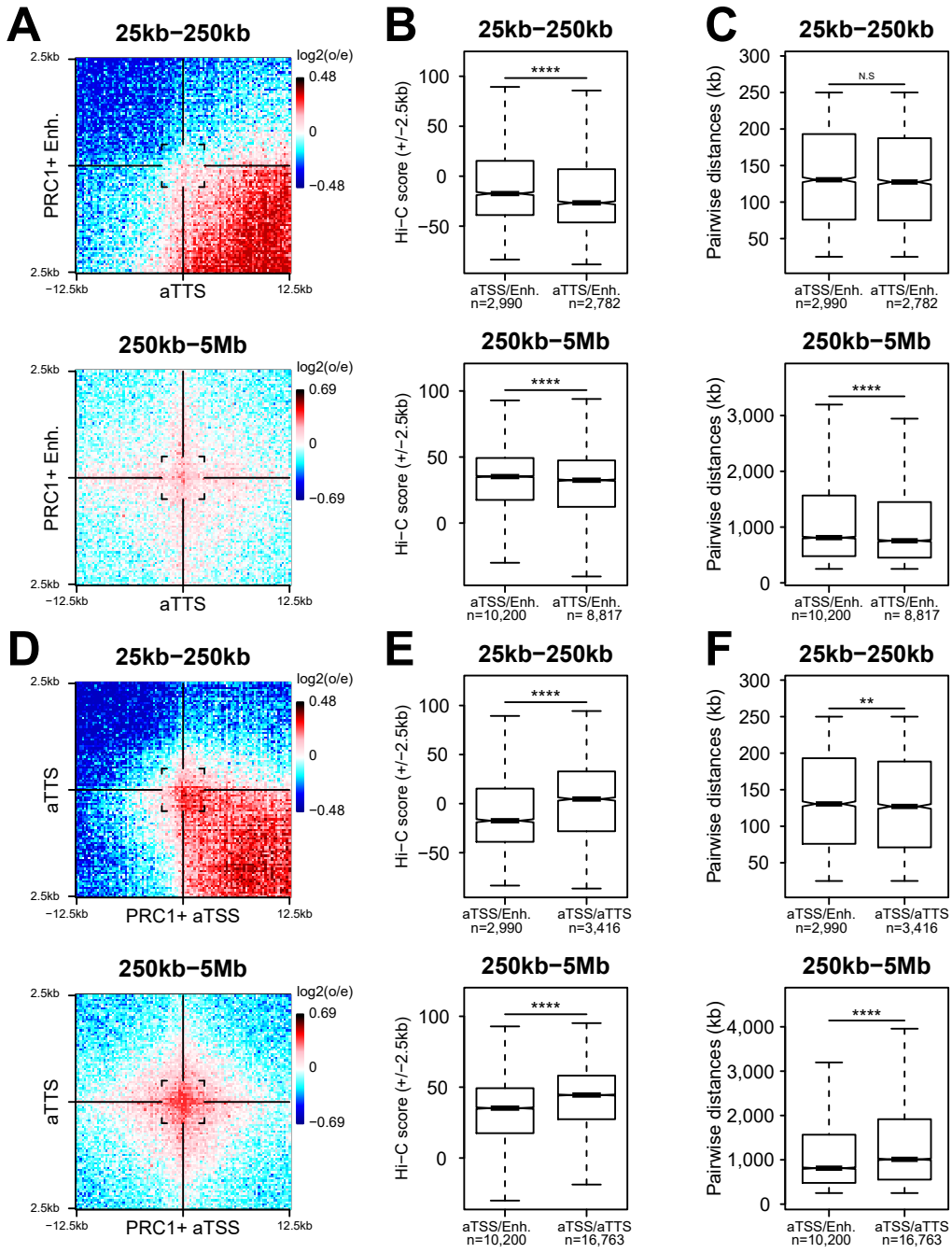
A
25kb−250kb
log2(o/e)
0.48
0
−0.48
2.5kb
PRC1+ Enh.
2.5kb
−12.5kb
aTTS
12.5kb
250kb−5Mb
log2(o/e)
0.69
0
−0.69
2.5kb
PRC1+ Enh.
2.5kb
−12.5kb
aTTS
12.5kb
B
25kb−250kb
Hi−C score (+/−2.5kb)
****
aTSS/Enh. n=2,990
aTTS/Enh. n=2,782
250kb−5Mb
Hi−C score (+/−2.5kb)
****
aTSS/Enh. n=10,200
aTTS/Enh. n= 8,817
C
25kb−250kb
Pairwise distances (kb)
N.S
aTSS/Enh. n=2,990
aTTS/Enh. n=2,782
250kb−5Mb
Pairwise distances (kb)
****
aTSS/Enh. n=10,200
aTTS/Enh. n= 8,817
D
25kb−250kb
log2(o/e)
0.48
0
−0.48
2.5kb
aTTS
2.5kb
−12.5kb
PRC1+ aTSS
12.5kb
250kb−5Mb
log2(o/e)
0.69
0
−0.69
2.5kb
aTTS
2.5kb
−12.5kb
PRC1+ aTSS
12.5kb
E
25kb−250kb
Hi−C score (+/−2.5kb)
****
aTSS/Enh. n=2,990
aTSS/aTTS n=3,416
250kb−5Mb
Hi−C score (+/−2.5kb)
****
aTSS/Enh. n=10,200
aTSS/aTTS n=16,763
F
25kb−250kb
Pairwise distances (kb)
**
aTSS/Enh. n=2,990
aTSS/aTTS n=3,416
250kb−5Mb
Pairwise distances (kb)
****
aTSS/Enh. n=10,200
aTSS/aTTS n=16,763

Figure S10

Fig. S10. PRC1-bound aTSSs form loops with the TTS of the corresponding genes, whereas PRC1-bound enhancers do not. A- Log2(observed/expected) aggregate interactions within 25kb windows centered on PRC1-bound enhancers (PRC1+ Enh.) and the Transcription Termination Sites (aTTSs) of the genes assigned to PRC1-bound aTSSs. No substantial interaction is detected at short- (25kb-250kb, top) or long-range distances (250kb-5Mb, bottom). **B-C-** Consistently, PRC1-anchored aTSS-enhancer loops show significantly stronger average Hi-C scores compared to the intersections of aTTSs and PRC1-bound enhancers (+/- 2.5kb) at both short- (top) and long-range (bottom) distances (B); although the former combination shows comparable (25kb-250kb, on the top) or significantly smaller (250kb-5Mb, on the bottom) pairwise distances (C). Wilcoxon p.val: **** < 1E-05; N.S: Not Significant. **D-F-** In comparison, PRC1-bound aTSSs contact the TTSs of corresponding genes at both short- and long-range distances (D-E), while displaying longer pairwise distances (F). Wilcoxon p.val: **** < 1E-05; ** < 1E-02.

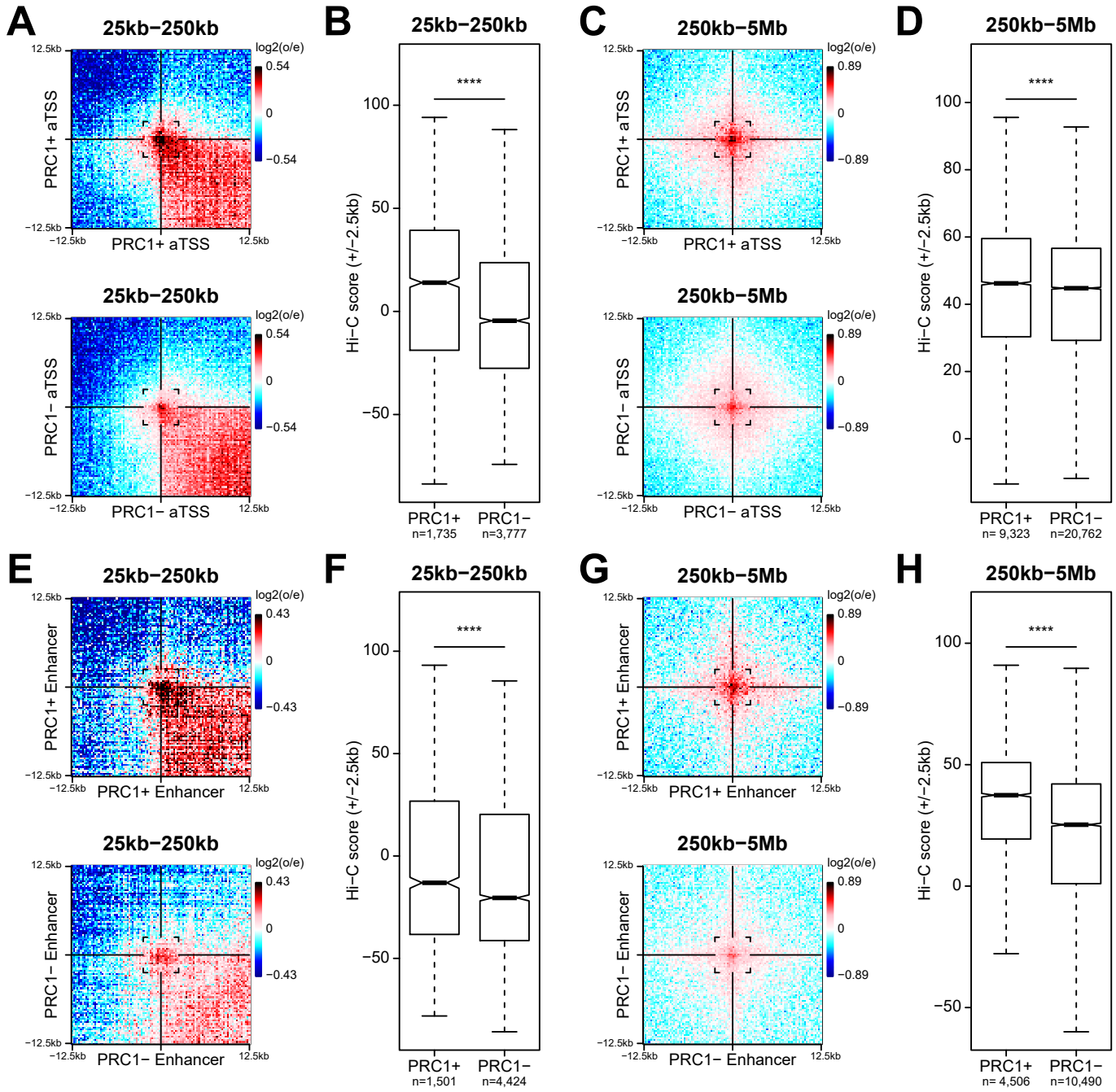
A
25kb−250kb
PRC1+ aTSS
PRC1+ aTSS
log2(o/e)
0.54
0
−0.54
12.5kb
−12.5kb
25kb−250kb
PRC1− aTSS
PRC1− aTSS
B
25kb−250kb
Hi−C score (+/−2.5kb)
****
PRC1+
n=1,735
PRC1−
n=3,777
C
250kb−5Mb
PRC1+ aTSS
PRC1+ aTSS
log2(o/e)
0.89
0
−0.89
250kb−5Mb
PRC1− aTSS
PRC1− aTSS
D
250kb−5Mb
Hi−C score (+/−2.5kb)
****
PRC1+
n= 9,323
PRC1−
n=20,762
E
25kb−250kb
PRC1+ Enhancer
PRC1+ Enhancer
log2(o/e)
0.43
0
−0.43
25kb−250kb
PRC1− Enhancer
PRC1− Enhancer
F
25kb−250kb
Hi−C score (+/−2.5kb)
****
PRC1+
n=1,501
PRC1−
n=4,424
G
250kb−5Mb
PRC1+ Enhancer
PRC1+ Enhancer
log2(o/e)
0.89
0
−0.89
250kb−5Mb
PRC1− Enhancer
PRC1− Enhancer
H
250kb−5Mb
Hi−C score (+/−2.5kb)
****
PRC1+
n= 4,506
PRC1−
n=10,490

Figure S11

Fig. S11. PRC1 binding is associated with increased aTSS-aTSS and enhancer-enhancer contact frequencies in ED. A-D- Log2(observed/expected) aggregate interactions within 25kb windows centered on PRC1-bound (PRC1+, upper panels) or PRC1-depleted (PRC1-, bottom panels) aTSS sites at short- (A, 25kb-250kb) and long-range (C, 250kb-5Mb) distances. Corresponding quantifications of the Hi-C score (+/- 2.5kb) are shown in B and D, respectively. Wilcoxon p.val: **** < 1E-05. Hence, contact frequencies between PRC1-bound aTSSs are significantly stronger compared to a control set of PRC1-depeleted aTSSs both at short- and long-range distances. **E-H-** Log2(observed/expected) aggregate interactions within 25kb windows centered on PRC1-bound (PRC1+, upper panels) or PRC1-depleted (PRC1-, bottom panels) enhancer sites at short- (E, 25kb-250kb) and long-range distances (G, 250kb-5Mb). Corresponding quantifications of the Hi-C score (+/- 2.5kb) are shown in F and H, respectively. Wilcoxon p.val: **** < 1E-05. Hence, contact frequencies between PRC1-bound enhancers are significantly stronger compared to a control set of PRC1-depeleted enhancers both at short- and long-range distances.

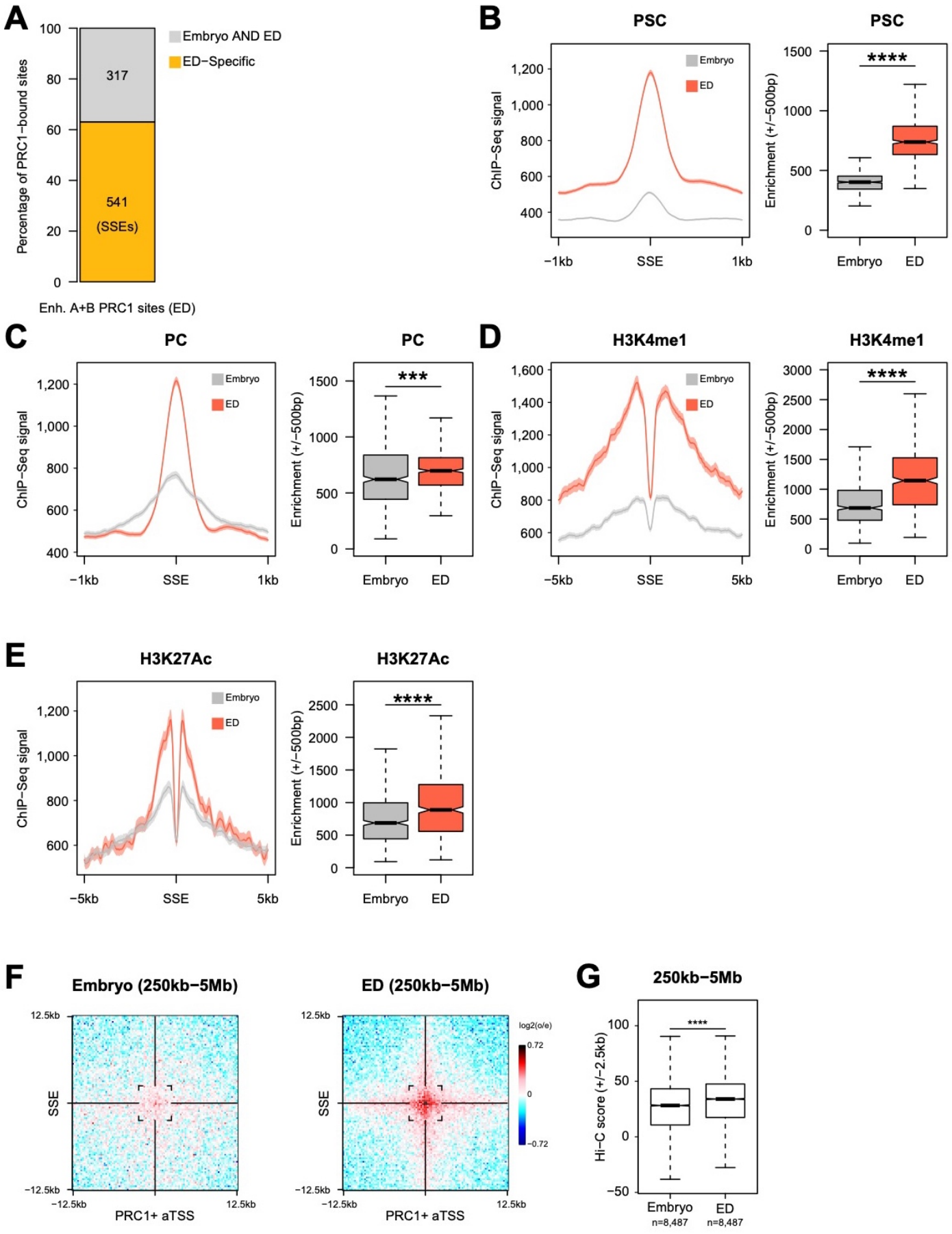
A
Embryo AND ED
ED−Specific
317
541
(SSEs)
Percentage of PRC1−bound sites
Enh. A+B PRC1 sites (ED)
B
PSC
PSC
Embryo
ED
ChIP−Seq signal
Enrichment (+/−500bp)
****
−1kb
SSE
1kb
C
PC
PC
***
D
H3K4me1
H3K4me1
****
−5kb
5kb
E
H3K27Ac
H3K27Ac
****
F
Embryo (250kb−5Mb)
ED (250kb−5Mb)
12.5kb
−12.5kb
SSE
PRC1+ aTSS
log2(o/e)
0.72
0
−0.72
G
250kb−5Mb
Hi−C score (+/−2.5kb)
n=8,487

Figure S12

Fig. S12. PRC1 redeployment at a subset of SSEs coincides with increased enhancer marks and enhancer-promoter contacts at the larval stage. A- Bar graph of the percentage of PRC1 enhancer sites (A+B) from ED that overlap with PRC1 peak summits (+/- 1kb) at the embryonic (in grey) and specifically at the larval stage (in yellow). The larval-specific enhancers (in yellow) were called Stage-Specific Enhancers (SSEs). **B-E-** Average ChIP-Seq tracks for the PRC1 proteins PSC (B) and PC (C), as well as the H3K4me1 (D) and H3K27Ac (E) enhancer marks around SSE sites at embryonic (in grey) and larval (in orange) stages. Corresponding quantifications (+/- 500bp) are shown on the right panels. Wilcoxon p.val: **** < 1E-05; *** < 1E-03. **F-G-** Log2(observed/expected) aggregate interactions within 25kb windows centered on PRC1-bound aTSSs (PRC1+ aTSS) and Stage-Specific Enhancer sites (SSE) at short- (25kb-250kb, on the left) and long-range (250kb-5Mb, on the right) distances in embryos (left) and ED (right). Corresponding quantifications of the Hi-C score (+/- 2.5kb) are shown in G. Wilcoxon p.val: **** < 1E-05.

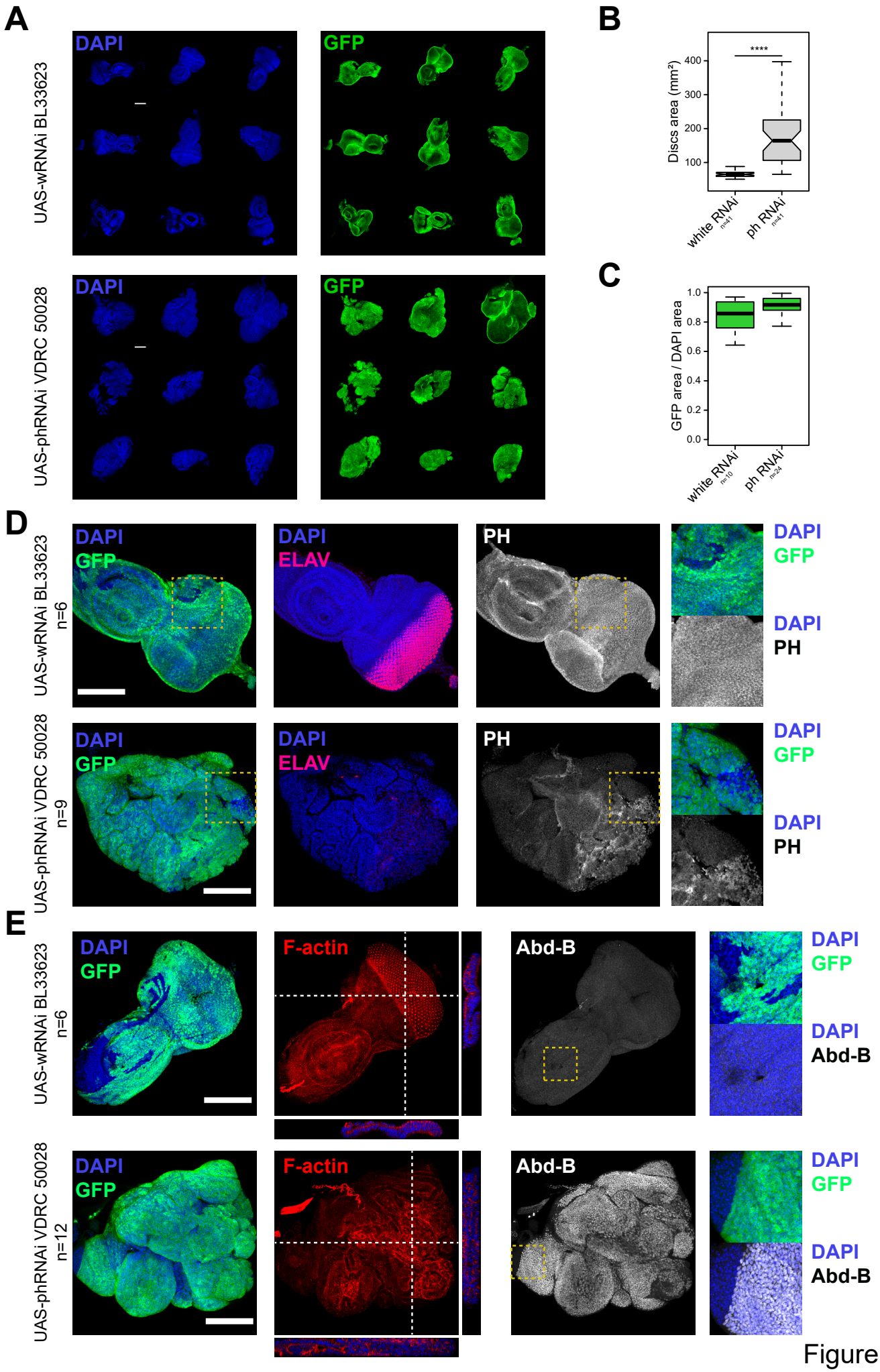
A
UAS-wRNAi BL33623
DAPI
GFP
UAS-phRNAi VDRC 50028
DAPI
GFP
B
Discs area (mm²)
400
300
200
100
****
white RNAi
n=41
ph RNAi
n=41
C
GFP area / DAPI area
1.0
0.8
0.6
0.4
0.2
0.0
white RNAi
n=10
ph RNAi
n=24
D
UAS-wRNAi BL33623
n=6
DAPI
GFP
DAPI
ELAV
PH
DAPI
GFP
DAPI
PH
UAS-phRNAi VDRC 50028
n=9
DAPI
GFP
DAPI
ELAV
PH
DAPI
GFP
DAPI
PH
E
UAS-wRNAi BL33623
n=6
DAPI
GFP
F-actin
Abd-B
DAPI
GFP
DAPI
Abd-B
UAS-phRNAi VDRC 50028
n=12
DAPI
GFP
F-actin
Abd-B
DAPI
GFP
DAPI
Abd-B

Figure S13

Fig. S13. UAS-*ph* RNAi clones phenocopy *ph* mutant clones. A- Representative DAPI (in blue) and GFP (in green) stainings of EDs bearing *white* RNAi (UAS-wRNAi, BL33623; top pannels) or *ph* RNAi (UAS-phRNAi, VDRC50028; bottom pannels) -expressing clones (GFP+). Scale bars: 100µm. **B-** Boxplot of the areas of EDs bearing *white* RNAi and *ph* RNAi clones. *ph*RNAi clones induce a major overgrowth of the tissue. Wilcoxon p.val: **** < 1E-05. **C-** Boxplot of the GFP+ clonal fraction in *white* RNAi and *ph* RNAi EDs (86% and 92%, respectively). **D-** DAPI (in blue), GFP (in green), ELAV (in red) and PH (in grey) immunostainings of *white* RNAi (top) and *ph* RNAi (bottom) clonal EDs. *ph* RNAi strongly reduces PH protein levels in a cell-autonomous fashion (see on the right, insets correspond to higher magnifications), as expected. Consistent with the tumor-suppressor role of *ph* in the ED, *ph* RNAi clones show impaired differentiation characterized by the loss of the ELAV neuronal differentiation marker (middle pannels). Scale bar: 100µm. **E-** DAPI (in blue), GFP (in green), F-actin (in red) and Abd-B (in grey) stainings of *white* RNAi (top) and *ph* RNAi (bottom) clonal EDs. *ph* RNAi impairs the apico-basal polarity of the ED epithelial cells (see orthogonal views for F-actin) and induces a strong, cell-autonomous derepression of the *Abdominal-B* homeotic gene (insets on the right correspond to higher magnification), as expected. Scale bar: 100µm.

A

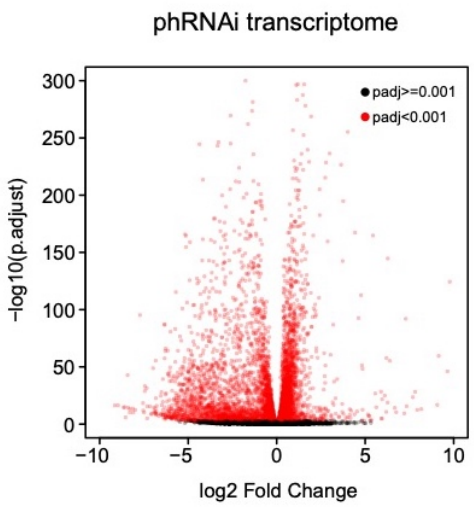

B

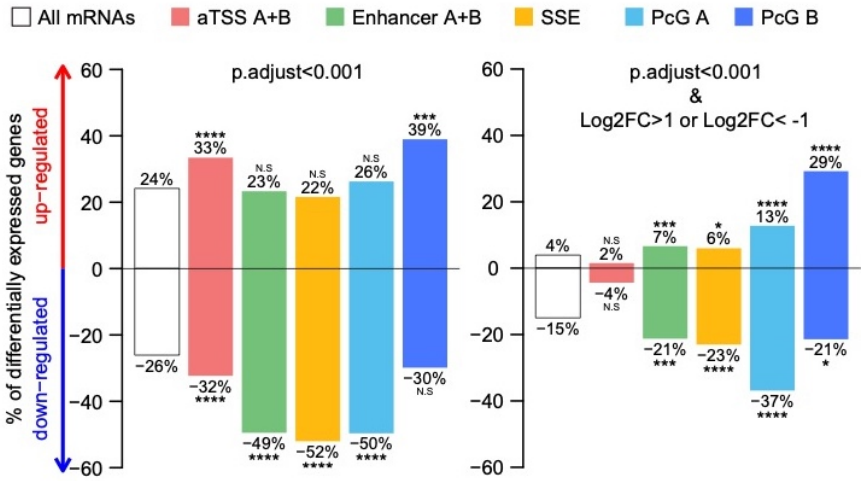

C

Symbol	Log2FoldChange	p.adjust
Abd−B	9.0	0.0e+00
Ubx	5.4	1.8e−165
ey	−2.4	6.0e−94
toy	−3.0	1.8e−50
dac	−1.1	9.4e−65
so	−3.6	1.4e−49
eyg	−0.6	4.8e−28
tsh	−1.7	1.3e−64
toe	−0.1	1.8e−01
dan	−2.1	3.1e−121
danr	−4.8	1.1e−23

Figure S14

Fig. S14. The transcriptional response to *ph* depletion varies upon chromatin types. A- Volcano plot of the *ph* RNAi vs *white* RNAi transcriptomes. Genes with a p.adjust smaller than 0.001 are shown in red. The overall transcriptome is unexpectedly skewed towards down-regulation. **B-** Percentage of significantly up- (top) and down- (bottom) regulated genes assigned to the aTSS A+B (red), Enhancer A+B (green), Stage-Specific Enhancers (yellow), PcG A (cyan) and PcG B (blue) clusters of PRC1 peaks (see Fig. 1H). As a control, the overall fraction of up- and down-regulated genes is shown in white. p.adjust and Log2FoldChange cutoffs are shown on the top. Hypergeometric test p.val: **** < 1E-05; *** < 1E-03; ** < 1E-02; * < 5E-02. **C-** Table depicting the Log2 Fold Change and the corresponding p.adjust for selected genes. The *Abdominal-B* (*Abd-B*) and *Ultrabithorax* (*Ubx*) homeotic are strongly derepressed, as expected, while most members of the Retinal Determination Gene Newtork (RDGN) are down-regulated, including *eyeless* (*ey*), *twin of eyeless* (*toy*), *dachsund* (*dac*), *sine oculis* (*so*), *eyegone* (*eyg*), *teashirt* (*tsh*), *distal antenna* (*dan*), and *distal antenna-related* (*danr*).

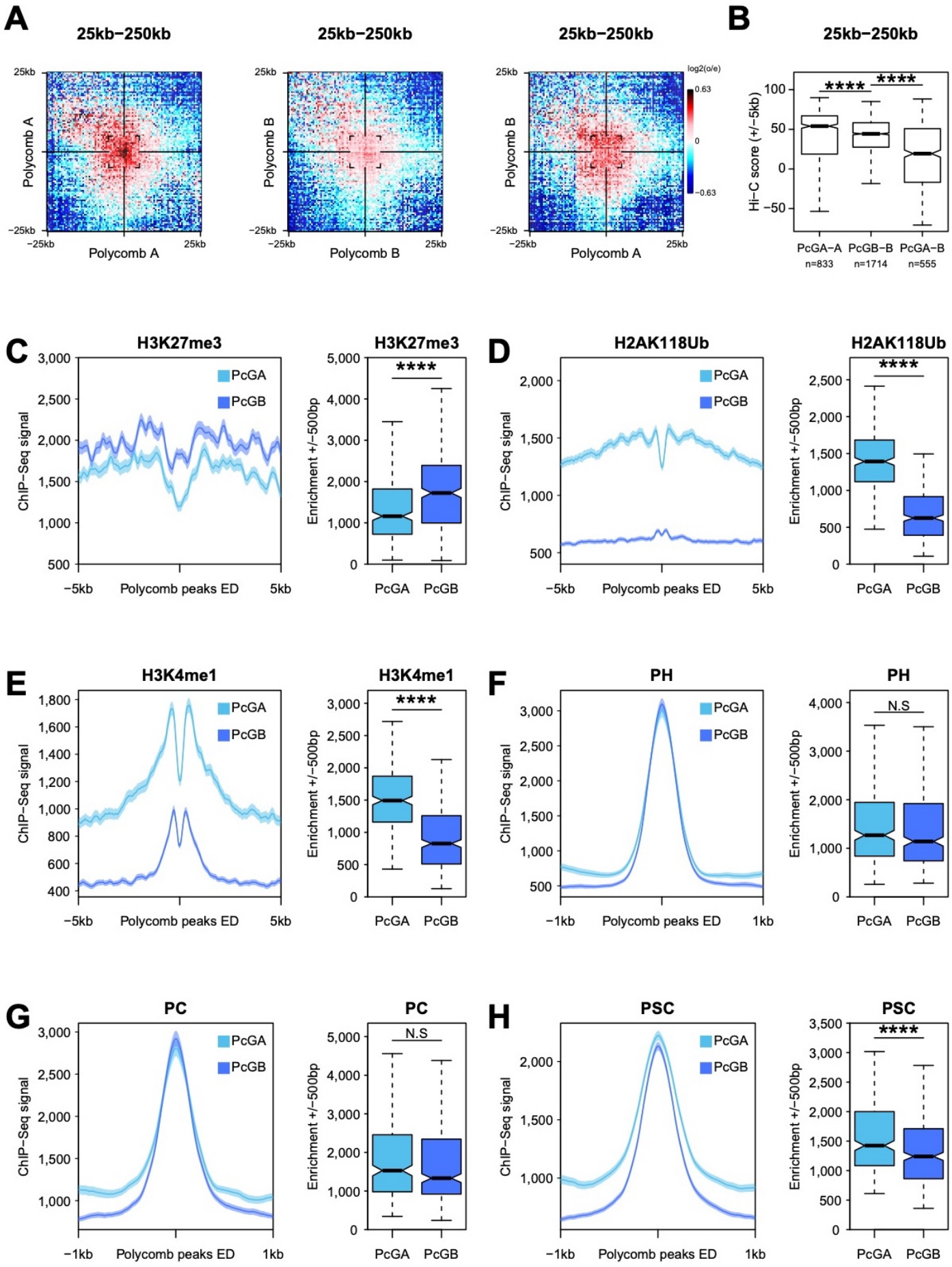
A
25kb−250kb
25kb−250kb
25kb−250kb
Polycomb A
Polycomb B
Polycomb A
Polycomb B
Polycomb B
Polycomb A
log2(o/e)
0.63
0
−0.63
B
25kb−250kb
Hi−C score (+/−5kb)
****
****
PcGA−A
PcGB−B
PcGA−B
n=833
n=1714
n=555
C
H3K27me3
H3K27me3
ChIP−Seq signal
Enrichment +/−500bp
PcGA
PcGB
Polycomb peaks ED
−5kb
5kb
****
D
H2AK118Ub
H2AK118Ub
E
H3K4me1
H3K4me1
F
PH
PH
N.S
G
PC
PC
N.S
H
PSC
PSC
−1kb
1kb

Figure S15

Fig. S15. Canonical Polycomb sites enriched for H2AK118Ub show higher H3K4me1 levels and higher contact frequencies in ED. A-B- Log2(observed/expected) aggregate interactions within 50kb windows between PRC1 peaks from the Polycomb A (enriched for both H3K27me3 and the PRC1-mediated H2AK118Ub marks, on the left), the Polycomb B (enriched for H3K27me3 but depleted for the H2AK118Ub mark, in the middle) or between Polycomb A and B (right) clusters of PRC1 peaks at short-range distances (25kb-250kb) in ED. Corresponding quantifications of the Hi-C score (+/- 5kb) are shown in B. **C-E-** Average ChIP-Seq tracks for the PRC2-mediated H3K27me3 (C), the PRC1-mediated H2AK118Ub (D) and the enhancer-related H3K4me1 (E) marks in ED centered on PRC1 peaks from the Polycomb A (in cyan) and Polycomb B (in blue) clusters (+/- 2.5kb). For each average track, the corresponding quantifications (+/- 500bp) are shown on the right part. The PRC1 peaks from the Polycomb A cluster show significantly higher H2AK118Ub and H3K4me1 levels and lower H3K27me3 compared to Polycomb B sites. **F-H-** Average ChIP-Seq tracks for the PRC1 proteins PH (F), PC (G) and PSC (H) centered on PRC1 peaks from the Polycomb A (in cyan) and Polycomb B (in blue) clusters (+/- 2.5kb). For each average track, quantifications are shown on the right part (+/- 500bp). The PRC1 peaks of the Polycomb A cluster show comparable PH and PC levels as well as higher PSC enrichments. Notably, H2AK118Ub-enriched PRC1 peaks (Polycomb A) show significantly higher contact frequencies compared to the H3K27me3-only PRC1 sites (Polycomb B). Wilcoxon p.val: **** < 1E-05; N.S: Not Significant.

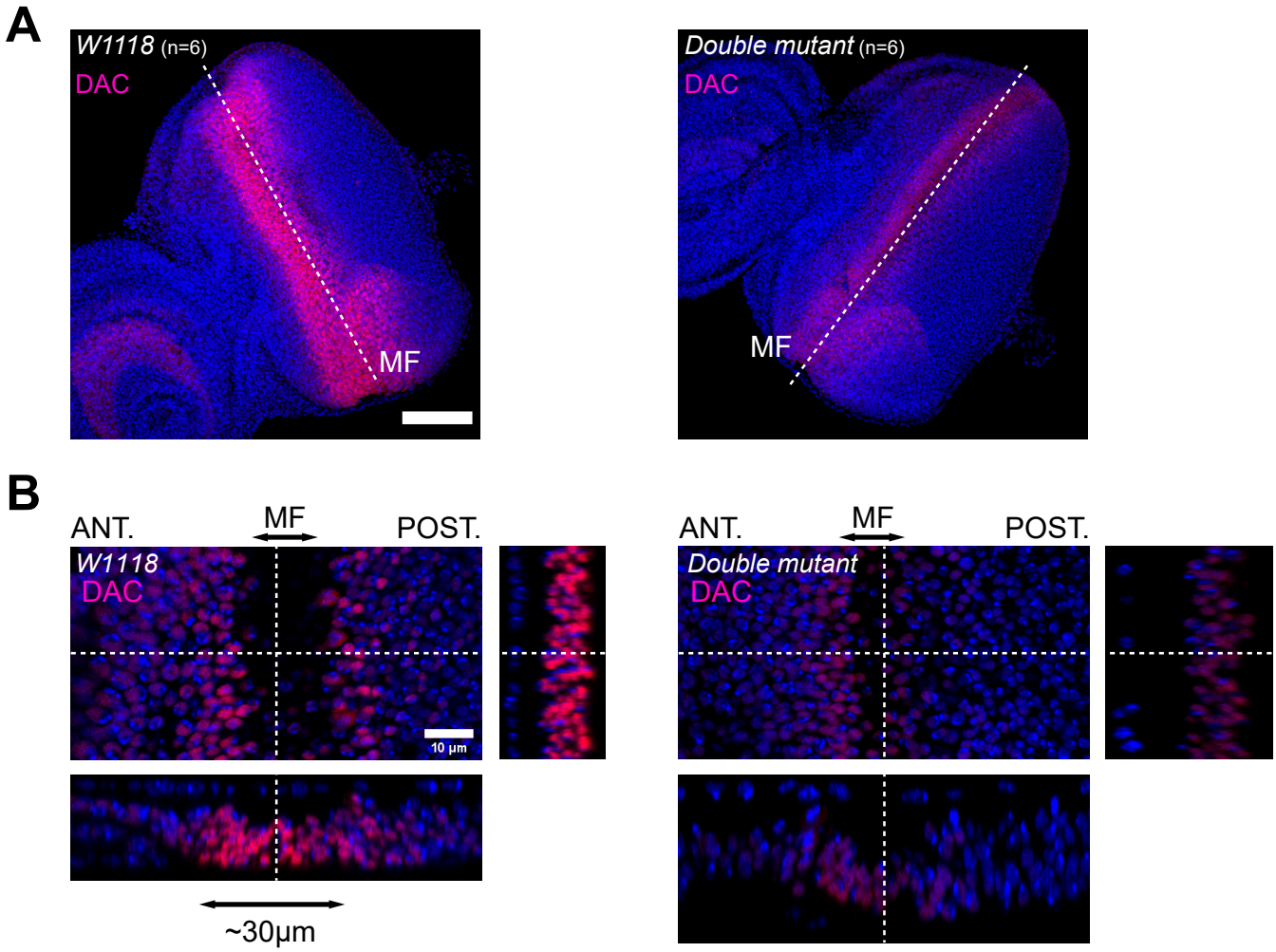
A
W1118 (n=6)
DAC
MF
Double mutant (n=6)
DAC
MF
B
ANT.
MF
POST.
W1118
DAC
10 µm
~30µm
ANT.
MF
POST.
Double mutant
DAC
C
CRISPR DELETIONS
16,400 kb
16,500 kb
Chr 2L
TSS-distal
TSS-proximal
FISH probes
PH ED
PC ED
PSC ED
H3K27me3 ED
[0 - 4,830]
[0 - 3,684]
[0 - 2,833]
[0 - 3,500]
CG5888
snoRNA:Me28S-A2958
ldgf1
ldgf2
ldgf3
dac
CG4580
Tpr2
CG5953
mir-494

Figure S16

Fig. S16. Removal of the two PRC1 anchors at the *dac* locus dampens its expression, while its expression pattern remains unchanged. A- Immunostaining of the DAC protein (in red) in WT (w^{1118}, left) and double mutant EDs (right). **B-** Centered view of the Morphogenetic Furrow (MF, indicated on the top) in WT (w^{1118}, left) and double mutant EDs (right). The DAC protein is detected in a restricted band of cells spanning the morphogenetic furrow. Removal of the two strong PRC1 binding sites in the vicinity of the *dac* locus (PRE mutant line) has a negative impact on DAC levels, while its expression pattern remains unaffected. Orthogonal views are shown on the bottom (xz) and the right (yz), and corresponding coordinates are projected on the picture (dashed lines). **C-** Screenshot of the *dac* locus. ChIP-Seq tracks for the PRC1 proteins PC, PH and PSC are shown in red, while the H3K27me3 ChIP-Seq track is in black. The sites excised using the CRISPR-Cas9 technology are indicated by dashed lines. Finally, the probes used for the 3D FISH of TSS-distal (left) and TSS-proximal (right) regions are shown in green and red, respectively.

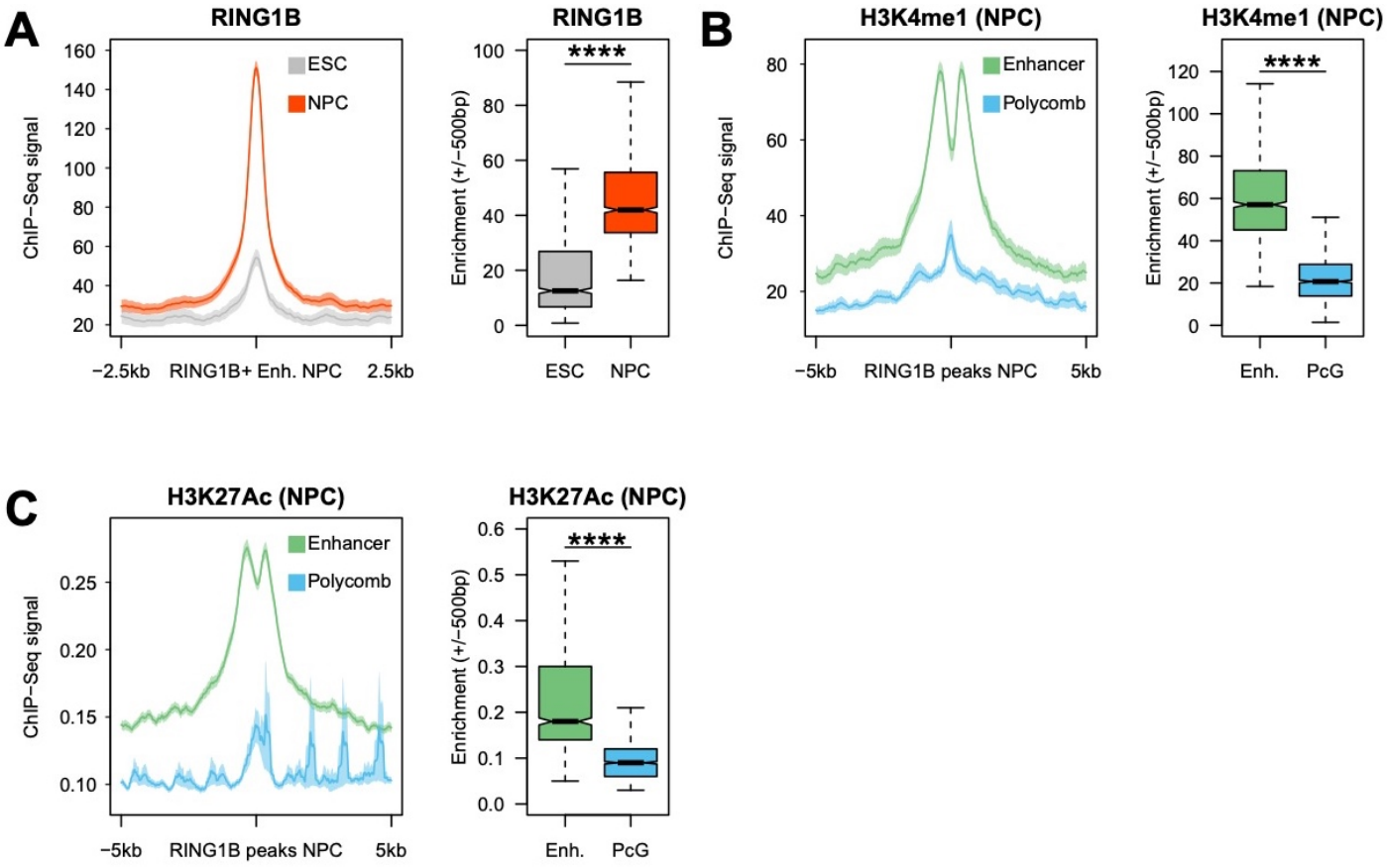
A
RING1B
ESC
NPC
ChIP−Seq signal
−2.5kb
RING1B+ Enh. NPC
2.5kb
RING1B
****
Enrichment (+/−500bp)
ESC
NPC
B
H3K4me1 (NPC)
Enhancer
Polycomb
ChIP−Seq signal
−5kb
RING1B peaks NPC
5kb
H3K4me1 (NPC)
****
Enrichment (+/−500bp)
Enh.
PcG
C
H3K27Ac (NPC)
Enhancer
Polycomb
ChIP−Seq signal
−5kb
RING1B peaks NPC
5kb
H3K27Ac (NPC)
****
Enrichment (+/−500bp)
Enh.
PcG

Figure S17

Fig. S17. RING1B is redeployed at active enhancer sites in NPCs. A- Average RING1B ChIP-Seq tracks from ESCs (in grey) and NPCs (in orange) centered on RING1B+ enhancer sites from NPCs (+/-2.5 kb). Corresponding quantifications (+/- 500bp) are shown on the right panel. RING1B binding at enhancer sites is markedly increased in NPCs. Wilcoxon p.val: **** < 1E-05. **B-C-** Average H3K4me1 and H3K27Ac ChIP-Seq tracks centered on RING1B peaks from the "enhancer" (in green) and "Polycomb" (in blue) clusters in NPCs. RING1B enhancer sites are enriched for the H3K4me1 and H3K27Ac active enhancer marks in NPCs. Corresponding quantifications are shown on the right (+/- 500bp). Wilcoxon p.val: **** < 1E-05; N.S: Not Significant.

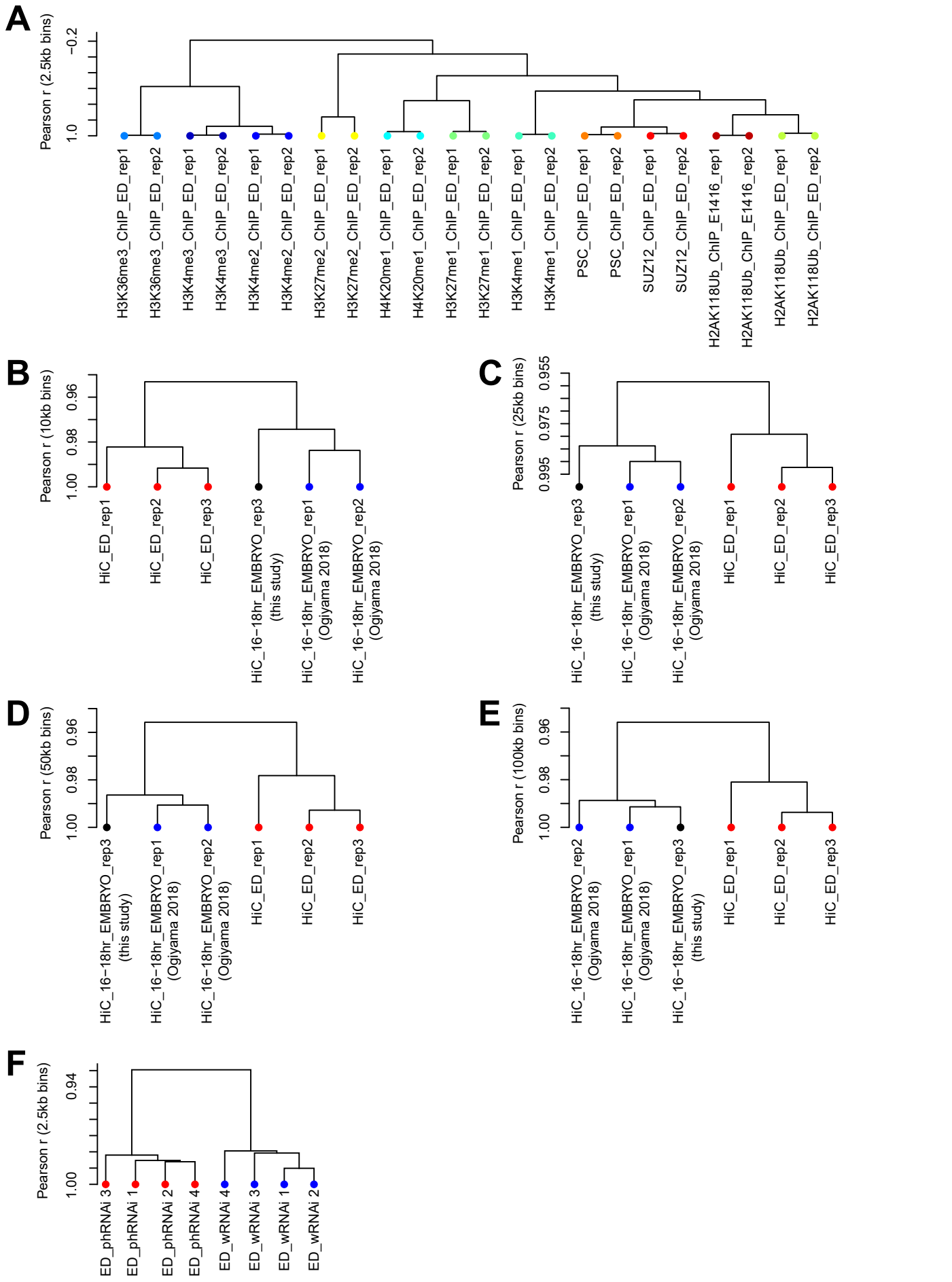
A
Pearson r (2.5kb bins)
1.0
−0.2
H3K36me3_ChIP_ED_rep1
H3K36me3_ChIP_ED_rep2
H3K4me3_ChIP_ED_rep1
H3K4me3_ChIP_ED_rep2
H3K4me2_ChIP_ED_rep1
H3K4me2_ChIP_ED_rep2
H3K27me2_ChIP_ED_rep1
H3K27me2_ChIP_ED_rep2
H4K20me1_ChIP_ED_rep1
H4K20me1_ChIP_ED_rep2
H3K27me1_ChIP_ED_rep1
H3K27me1_ChIP_ED_rep2
H3K4me1_ChIP_ED_rep1
H3K4me1_ChIP_ED_rep2
PSC_ChIP_ED_rep1
PSC_ChIP_ED_rep2
SUZ12_ChIP_ED_rep1
SUZ12_ChIP_ED_rep2
H2AK118Ub_ChIP_E1416_rep1
H2AK118Ub_ChIP_E1416_rep2
H2AK118Ub_ChIP_ED_rep1
H2AK118Ub_ChIP_ED_rep2
B
Pearson r (10kb bins)
1.00
0.98
0.96
HiC_ED_rep1
HiC_ED_rep2
HiC_ED_rep3
HiC_16−18hr_EMBRYO_rep3 (this study)
HiC_16−18hr_EMBRYO_rep1 (Ogiyama 2018)
HiC_16−18hr_EMBRYO_rep2 (Ogiyama 2018)
C
Pearson r (25kb bins)
0.995
0.975
0.955
HiC_16−18hr_EMBRYO_rep3 (this study)
HiC_16−18hr_EMBRYO_rep1 (Ogiyama 2018)
HiC_16−18hr_EMBRYO_rep2 (Ogiyama 2018)
HiC_ED_rep1
HiC_ED_rep2
HiC_ED_rep3
D
Pearson r (50kb bins)
1.00
0.98
0.96
HiC_16−18hr_EMBRYO_rep3 (this study)
HiC_16−18hr_EMBRYO_rep1 (Ogiyama 2018)
HiC_16−18hr_EMBRYO_rep2 (Ogiyama 2018)
HiC_ED_rep1
HiC_ED_rep2
HiC_ED_rep3
E
Pearson r (100kb bins)
1.00
0.98
0.96
HiC_16−18hr_EMBRYO_rep2 (Ogiyama 2018)
HiC_16−18hr_EMBRYO_rep1 (Ogiyama 2018)
HiC_16−18hr_EMBRYO_rep3 (this study)
HiC_ED_rep1
HiC_ED_rep2
HiC_ED_rep3
F
Pearson r (2.5kb bins)
1.00
0.94
ED_phRNAi 3
ED_phRNAi 1
ED_phRNAi 2
ED_phRNAi 4
ED_wRNAi 4
ED_wRNAi 3
ED_wRNAi 1
ED_wRNAi 2

Figure S18

Fig. S18. Clustering of ChIP-seq and Hi-C replicates from ED and whole *Drosophila* embryos. A- Clustering of the ChIP-Seq replicates generated in this study based on Pearson Correlation Coefficients. **B-E-** Clustering of the Hi-C replicates from ED (red) and whole 16-18h embryo (in black) generated in this study using different bin sizes (see on the y axis of each plot). The two Hi-C replicates generated by Ogiyama et al., 2018 from whole 16-18h embryo using the same protocol (in blue) do cluster with our newly generated Hi-C from embryos (in black). Hence, the three replicates were merged to increase the resolution of the maps (fig. S1). **F-** Clustering of the *white* RNAi and *ph* RNAi RNA-Seq replicates based on Pearson Correlation Coefficients.